J Intell Manuf (2019) 30:833–854
https://doi.org/10.1007/s10845-016-1285-z

Working parameter optimization of strengthen waterjet grinding with the orthogonal-experiment-design-based ANFIS

Zhongwei Liang[1,2] · **Shaopeng Liao**[1,2] · **Yiheng Wen**[1,2] · **Xiaochu Liu**[1,2]

Received: 27 February 2016 / Accepted: 22 November 2016 / Published online: 2 December 2016

Abstract In this paper, the working parameter optimization of strengthen waterjet grinding by employing the orthogonal-experiment-design-based ANFIS (Adaptive Neural Fuzzy Inference System), was conducted to obtain an optimal result of bearing ring machining. An improved ANFIS system based upon orthogonal experiment design, was proposed to optimize the working parameters in grinding practices, which increases the surface hardness of ring surface from 49.0 to 72.0 HRC, topography elasticity variance from 330.0 to 670.0, texture energy from 24.5 to 88.0, decreases the surface roughness from 0.65 to 0.25 μm, and loading deviation from 1860.5 to 1320.0, thereafter an optimal grinding quality can be obtained. The optimization approach proposed involve the following steps: Preparation of experimental environment; Measure index determination for ring surface; Orthogonal experiment design for making fuzzy logic rules; Establishment of ANFIS system; Working parameter optimization for waterjet grinding; and Performance verification for actual grinding. Objective of this research is determining the optimal working parameters with fewer experimental iterations compared to other alternative approaches, such as Genetic parameter optimization, SA–GA parametric prediction, Taguchi parameter estimation, ANN–SA parametric selection, and GONNs parameter selection method. Statistical analysis and result comparisons support its efficiency and reliability in machining practices, a stable and reliable grinding process can be achieved for typical conditions by using waterjet pressure at around 310 MPa, flow rates of water mass at about 5.8 kg/min, attack angle by 60–75°, mass rate of abrasive grit by about 0.4 kg/min, and traverse speed by 60 mm/min. It was concluded that this proposed ANFIS system can be used as a suitable and effective tool, to investigate the complicated influential correlation between waterjet working parameters and grinding effectiveness in bearing manufacturing, and to give a better machining performance compared to other experimental practices.

Keywords Working parameter · Optimization · Strengthen waterjet grinding · Orthogonal experiment design · ANFIS

Part I: Fundamental preparation for experiment

Introduction

Strengthen waterjet grinding is a rapidly developing technology used for a number of applications including plate profiling and engineering material machining. During this process, the mixed water-based abrasive slurry was coverage sprayed on the specimen workpiece surface by the speed of 100–300 m/s and in the jet angle of 15–75°, therefore a continuous violent collision happens between abrasive grits or steel particles and objective surface to be machined, makes the lattice relaxation and structure cracking of metal atoms, thereafter plasma region emerges by a high-energy electron excitation, thus tribo-chemical reaction induced between strengthen grinding modified liquid and metal material, which improves machining quality and releases surface residual stress in return.

The important working parameters of waterjet grinding can be categorized as Hydraulic parameters: water pressure

✉ Zhongwei Liang
lzwstalin@126.com

[1] School of Mechanical and Electrical Engineering, Guangzhou University, Guangzhou 510006, People's Republic of China

[2] The Guangzhou Key Laboratory for Strengthen Grinding and High Performance Machining of Metal Material, Guangzhou University, Guangzhou 510006, People's Republic of China

and water flow rate; Abrasive parameters: abrasive type, grit size, grit shape, mass rate of abrasive grits; Machining parameters: traverse rate, stand-off-distance (SOD), number of passes, attack angle, targeted surface material; and Mixing parameters: mixing method (forced or suction), abrasive condition (dry or slurry), mixing chamber dimensions. Varieties of materials that can be machined by waterjet grinding include copper and metal alloys, aluminum, lead, steel, tungsten carbide, titanium, etc. Best of waterjet machining processes rely on grit- impacting action of abrasive laden waterjet for the applications of cutting, grinding, polishing, cleaning, and decaling of thick sections of very soft to very hard materials at higher rates (Liang et al. 2013). A stream of small abrasive grits introduced and entrained by waterjet in such a manner that the momentum of waterjet was partly transferred to abrasive grits. The primarily role of carrier fluid (water) is to accelerate large quantities of abrasive grits to a high velocity and to produce a highly coherent jet.

Resulting from the rapid progresses of AWJ (Abrasive Waterjet) grinding, the complexity and depth of its research outperformed the classical machining comparisons or purely process simulations already (Axinte et al. 2009). Simultaneously, the monitory of high-speed waterjet grinding or material removal touches upon the influence mechanism of performance optimization, especially the working parameter optimization during waterjet grinding should be emphasized by higher attention, cause it presents an obvious impact upon the following topographic shaping and mechanical characteristics of specimen workpiece surface. Although current machining researches provide crucial theoretical foundations and scientific supports to select working parameters in practices, most of them cannot offer quantitative tools to realize grinding optimization successfully.

Considering the research results about waterjet grinding, some original ideas focused on energy beam powered already (Bilbao Guillerna et al. 2015); meanwhile, an improvement model of profiling or dressing the grinding wheels was proposed (Axinte et al. 2009). For instance, Schwartzentruber and Papini (2015) studied on the abrasive waterjet micropiercing of borosilicate glass. Besides, Chen and Jiang (2015) proposed a force controlled grinding-milling technique for quartz-glass micromachining. Simultaneously, Srinivasu and Axinte (2014) reported their latest progresses on the surface integrity analysis of plain-waterjet-milled engineering composite materials. These works provide valuable scientific references for machining investigations in different experimental conditions, but a detailed and systematic analysis concerning with grinding optimization, not just traditional process monitory characterized by purely machining tests or directly calibration with machined results, still not been studied in-depth yet, which undoubtedly weakens waterjet grinding researches in accuracy and reliability.

Furthermore, on the topic of ANFIS optimization in waterjet grinding, Maher et al. (2015) improved wire EDM (Electrical Discharge Machining) performance at different machining parameters by ANFIS modeling; a developed ANFIS system can eliminate the need of extensive experimental work, for selecting the most effectively grinding parameters (Sarkheyli et al. 2015; Al-Ghamdi and Taylan 2015); Abdulshahed et al. (2015a), Abdulshahed et al. (2015b) and Phootrakornchai and Jiriwibhakorn (2015) respectively focused on the application of ANFIS prediction for thermal error compensation on CNC machine tools, and on the online critical clearing time estimation as well. More relevant researches on the ANFIS application in machining operation can be found from the published literature (Abhishek et al. 2014; Prakash et al. 2014) also. When discussing the monitoring of tool wear by using measured machining forces and neuro-fuzzy modelling approaches during the machining process of GFRP (Glass Fibre Reinforced Polymer) composites, Azmi (2015) has made a detailed report. Meanwhile, literatures (Shabgard et al. 2013; Labib et al. 2011) published their latest researches on the fuzzy logic control of EDM. As they paid high attentions on the fuzzy analysis between the experimental results and the influence factors of strengthen waterjet machining, it should be regrettably pointed out that they hardly cover all involved participant elements in grinding operation, from the selection of grinding parameters to the resultant grinding optimization.

As orthogonal experiment provides a useful tool to study machining process and obtained results in a more effective and accurate way, Fan et al. (2015) made orthogonal experiments on the direct reduction of carbon-bearing pellets of bayer red mud. Besides, He et al. (2015) have made a tribilogical performance of connecting rod by using orthogonal experiment. Thereafter, Zhang et al. (2015) reported their latest progresses on the deposition parameters in the synthesis of CVD (Chemical Vapor Deposition) microcrystalline diamond powders, which optimized by orthogonal experiment design. Other similar literatures can be learned from Lee et al. (2013), Gao et al. (2012) Nagesh et al. (2015), Dong et al. (2010) also. There is still few published literature focus on orthogonal experiment design for waterjet grinding evaluation or parameter optimization; thereafter, some fundamental questions concerning about its quantitative comparison and mutual- influence identification remain unaddressed, which makes the systematic research on these theoretical domains need to be improved and focused further.

This paper was structured as follows: Firstly, “Introduction” section outlines the importance and necessity of investigating the parameter optimization of strengthen waterjet grinding, based on the orthogonal-experiment-design-based ANFIS; “Establishment of experimental environment” section discusses the establishment of experimental environment; “Measure indexes characterizing the bearing ring

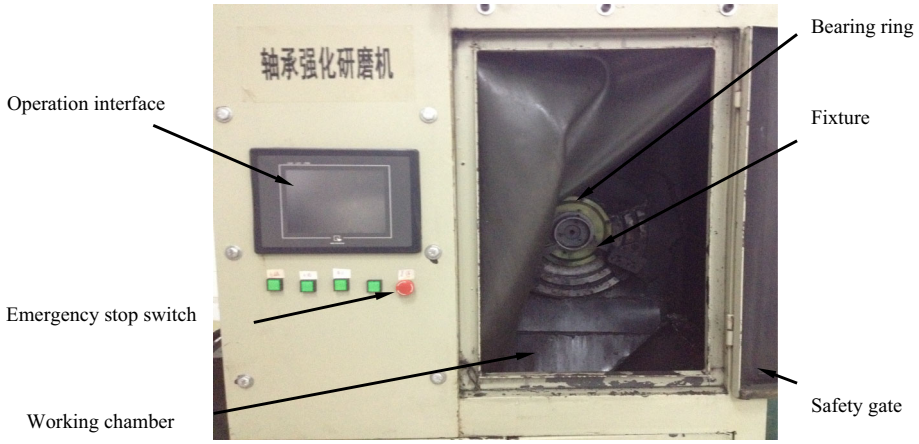

Fig. 1 General structure of grinding machine

surface" section proposes a series of measure indexes characterizing the bearing ring surface, and "Theory of the orthogonal-experiment-design-based ANFIS" section explains the theory of ANFIS; then, "Application of ANFIS optimization" section presents the application process of ANFIS optimization in details. Finally, based on the all-around optimization analysis and performance discussions of this new approach in "Optimization results and performance discussions" and "Conclusions" sections concludes this paper as required.

Establishment of experimental environment

Figure 1 shows the general structure of waterjet grinding machine used. The experimental set-up was consisted by a high-performance intensifier pump and a 6-freedom-degree device fitted with the high-pressure waterjet accessories, receiver and abrasive feeding/mass flow monitory system. The intensifier was capable of supplying water up to a maximum pressure of 55,000 psi (380 MPa), while the device was used to position and move the nozzle in order to carry out the strengthen grinding operation. Water was pumped to waterjet system via an air-driven water pump, Haskel ASF-60, and its pressure was stabilized by an accumulator. Thereafter the pressurized water was delivered to a pressure tank where water squeezed into a built-in confined box containing pre-mixed abrasive slurry. The box was made of steel for isolating the abrasive slurry from the incoming water. By this arrangement, it ensured that the abrasive grit concentration was controllable and maintained constantly. The pressure tank was mounted on a shaker vibrating at about 1–5 Hz to allow abrasive grits uniformly distributed within the slurry mixture inside the whole confined box (Mohamad et al. 2015). Figure 2 illustrates the setup of waterjet grinding operation and the measured topography of ring surface, its inner structure can be learned from Fig. 3.

In this experimental set-up, filtrated water was pressurized and then forced through a ruby orifice that makes the jet travel to the nozzle body for creating a partial vacuum through the abrasive inlet. Abrasive grits were accelerated by jet energy in mixing/focusing tube to form high-speed abrasive waterjet. Although the full capacity of waterjet system reaches 380 MPa, a much lower water pressure was used with selected feed rates to make sure that the shallow depths of grinding operation can be observed for performance optimization and process monitoring. A high nozzle ratio (length to diameter) allows an effective isolation of upstream disturbance in jet flow. Nozzle was mounted to a computer controlled x–y–z stage, with the control resolution by 0.01 mm. While the machine was used to position and move the nozzle in order to carry out the grinding operation, it was programmed to execute the linear (traverse speed) motion of nozzle head in given sequence (Jia et al. 2013). The ring specimen to be machined was mounted horizontally with its surface perpendicular to the vertically placed waterjet axis and the nozzle tube moved over it. This arrangement allows abrasive waterjet to be drained out of the workpiece specimen by gravity to reduce the likelihood of building up of slurry layers on the machined surface. Figure 4 shows the objective bearing rings to be machined, Table 1 gives the key parameters of experimental device set-up.

The outside surface of bearing ring (AISI52100 or GC_r15) was used as workpiece specimen for grinding research. As waterjet grinding involves a large number of influential variables, only those major and controllable dynamic ones were considered in this study, including waterjet pressure (P_w/MPa), mass flow rates (F_r/ kg/min), waterjet attack angle (W_a/°), mass rate of abrasive grit (F_a/kg/min), and traverse speed (T_s/mm/min), while others keeping constant, as shown by Table 2. To ensure the high repeatability of testing conditions, following conditions should be met in advance: Abrasive mass flow was delivered by a controlled mechanical metering system and calibrated before each test; the feed speed of jet flow was monitored on line via signal

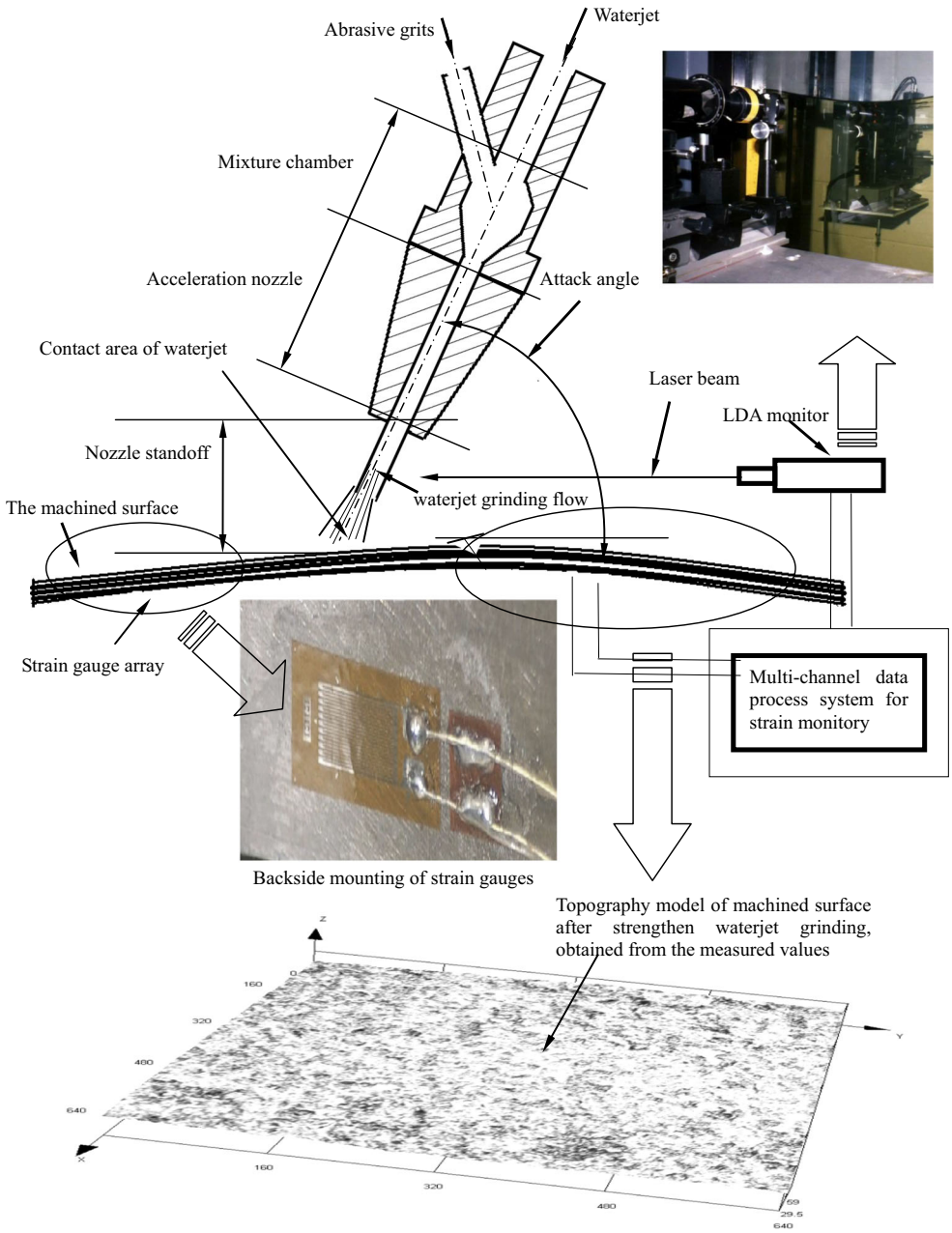

Fig. 2 Operation mechanism of waterjet grinding monitory and three-dimensional topography model after strengthen waterjet grinding

acquisition from the computerized quadratic encoder (Yusup et al. 2014). Besides, computer software with graphic interface was used for the control of data collection, online fusion and data display (Liang et al. 2013). The dynamometer was connected to a 3-channel charge amplifier type through a connecting cable type, which in turn connected to PC by a 37-pin cable from A/D board. Based on these preparations, a computer-controlled data acquisition system was used to collect and record the measured index from grinding experiments.

Measure indexes characterizing the bearing ring surface

As the surface topography of bearing ring can be approximated accurately by spatial geometric surface, except some frequently-used indexes, such as *Surface hardness* (H_v) and *Surface roughness* (R_a), the following physical indexes were proposed also by reference to free-form surfacing model, in the desire of describing topography more reliably (Hayasi and Asiabanpour 2013):

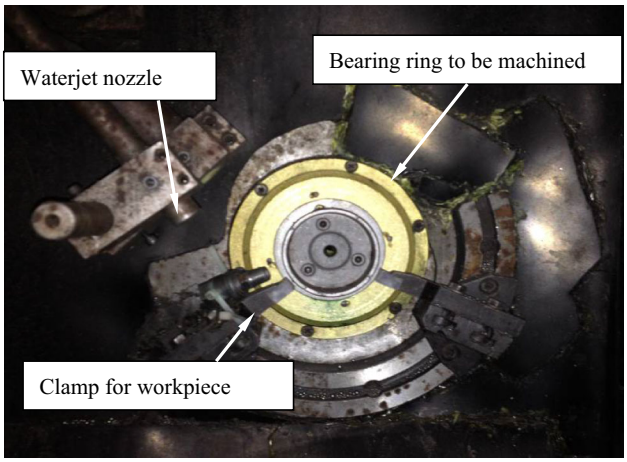

Fig. 3 The inner structure of waterjet grinding machine

Fig. 4 Objective bearing rings to be machined

Table 1 Key parameters of experimental device set-up

Working parameters	Value and units
Nozzle/orifice diameter	0.5 mm
Diameter of abrasive powder	150–300 μm
Experimental temperature	26°
Measuring time interval	90 μm
Cutting speed on surface	10 m/min
Penetration depth into material	2.5 mm
Experimental device size	1400 mm × 1000 mm × 2000 mm

Topography elasticity variance (T_v): Surface elasticity demonstrates the transformation-resisting capability of spatial surface shape under external force loading, it becomes a typical index to calibrate shape characteristics in coordinate system, simultaneously surface elasticity shows the concentricity level of characteristic distribution in elasticity values as well. In this experiment, elasticity variance denotes the elasticity distribution of certain topography section, which

Table 2 Working parameters used in strengthen waterjet grinding

Working parameter	Value
Waterjet pressure (P_w)	250–350 (MPa)
Flow rates of water mass (F_r)	2.5–7.5 (kg/min)
Waterjet attack angle (W_a)	35°–85°
Mass rate of abrasive grit (F_a)	0.30–0.50 (kg/min)
Enhanced liquid: Tri-ethanolamine solution; AES resin; water	
Traverse speed (T_s)	20–70 (mm/min)

makes it conveniently used to illustrate topography characteristics from the perspective of elasticity variance:

$$\varphi = \alpha_1 \sum_{i=1}^{m} W_{ui}^2 + \beta_1 \sum_{i=1}^{m} W_{uui}^2 + \alpha_2 \sum_{j=1}^{n} W_{vj}^2 + \beta_2 \sum_{j=1}^{n} W_{vvj}^2 + \alpha_1\alpha_2\beta_1\beta_2 \sum_{i=1}^{m}\sum_{j=1}^{n} W_{uivj}^2 - 2f(u,v)W$$

Here W denotes objective ring topography in the form of B-spline basis function; W_u, W_v, W_{uu}, W_{vv}, W_{uv} are the partial derivatives of W in the first order, second order and hybrid state in u, v axes respectively; $\alpha_1, \alpha_2, \beta_1, \beta_2$ are the given coefficients, $f(u, v)$ denotes a given function of surface vector, m, n denote the order amounts of surface vector in u, v axes.

Texture energy (T_e): Texture energy of surface plays a prominent role as fairness function in the occasions of geometric modeling or micro-characteristic surface analysis. Therefore the distribution of surface energy can be computed and quantified to denote its belonged experimental conditions and geometric characteristics. This measure index was defined as the scatter level of texture energy in mathematical sense, for a high value shows a more decentralized scattering of texture energy in fitted ring surfaces:

$$\begin{aligned}\zeta = &\sum_{i=1}^{m} \int_{\Omega} S_u(u_i)^2 du \\ &+ \sum_{i=1}^{m}\sum_{i=1}^{m} \iint_{i\in\Omega} S_{uu}(u_{ii})^2 du du + \sum_{j=1}^{n} \int_{\Omega} S_v(v_j)^2 dv \\ &+ \sum_{j=1}^{n}\sum_{j=1}^{n} \iint_{j\in\Omega} S_{vv}(v_{jj})^2 dv dv \\ &+ \sum_{i=1}^{m}\sum_{j=1}^{n} \iint_{\Omega} S_{uv}(u_i v_j)^2 du dv \end{aligned} \quad (1)$$

Here $S_u(u_i)$, $S_{uu}(u_{ii})$, $S_v(v_j)$, $S_{vv}(v_{jj})$, $S_{uv}(u_i v_j)$ denoted as the first order, second order and hybrid derivatives of

objective ring surface $f(u, v)$ in the directions of u, v axes respectively.

Loading deviation of surface topography (L_d): Since surface construction highly depends on external loading such as mechanical force and inertia moment, the constructed topography results will be deformed in an obviously scale. For the purpose of showing and quantifying the influential effects caused from external waterjet force loading, this measure index was proposed to calibrate the difference deviation and variation principle between the forced and original surface topography of ring periphery, as a high value demonstrates a relative-critically deformation of resultant surface topography, with the definition shown as:

$$\rho = -2 \sum_{i=0,m_u}^{u} \sum_{j=0.m_v}^{v} V_{i,j} \oiint_{i,j\in\Omega} N_{i,s_u}(u) \times N_{j,s_v}(v) N_{i,j}(uv) f(u, v) du dv \tag{2}$$

Here $N_{i,su}(u)$, $N_{j,sv}(v)$, $N_{i,j}(uv)$ denote the boundary-controlled B-spline surfaces in *u,v,uv* axis respectively, $V_{i,j}$ denotes the transitional vector between two adjacent topographic control vertexes impacted by external loading of the grinded surface to be investigated.

In order to obtain the detailed measure indexes from the ring surface to be machined, its periphery has been sampled by 12 measure points for property measurements, as demonstrated by Fig. 5. A set of FESEM (Field Emission Scanning Electron Microscopy) has been used to observe the differences on ring surface micro-topography before and after waterjet grinding, while surface roughness can be measured by TIME 3230 roughness measuring instrument for the sake of following data analysis. The mean values were averaged by three measurement cycles from these 12 measure points on ring surface periphery.

$$\text{Measure\_Index}^{(k)}_{\text{mean value}} = \frac{\sum_{i=1}^{3}\left[\sum_{j=1}^{12} \text{Measure\_Index}^{(k)}{}_{(i,j)}\right]}{3 \times 12} \tag{3}$$

Here $Measure\_Index^{(k)}_{mean\ value}$ denotes the mathematical averages of objective measure indexes ($Measure\_Index^{(k)}_{(i,j)}$) on ring periphery, as k denotes H_v, R_a, T_v, T_e and L_d respectively; $i = 1, 2, 3$ shows the measurement cycles, and $j = 1, 2, \ldots, 12$ denotes the targeted measure point on ring periphery, on which the measurements of topography properties were carried out. Experiments were repeated four times to circumvent all possible errors, therefore a total of 144 measurements should be conducted. In each sampled area the distance from the highest value peak to the deepest value valley was recorded then the averages of them can be taken. Figures 6, 7, 8, 9, and 10 show the mean value comparisons of H_v, R_a, T_v, T_e, L_d grouped from A to J.

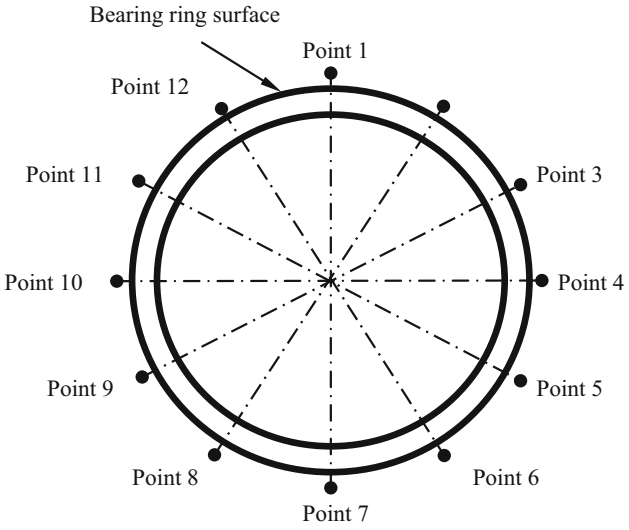

Fig. 5 Periphery distribution of measure points on bearing ring surface

Theory of the orthogonal-experiment-design-based ANFIS

In this section the basic theory of an improved adaptive neural fuzzy inference network (ANFIS) was presented. As fuzzy theory is one of the most important mathematical theories and can be used effectively for the uncertainty, multi-input and discrete data sets, ANFIS optimization becomes an absolute measurement of the data differences between those participant parameter sequences, and is also used to inspect an approximate classification between black and white conditions (Sedighi and Afshari 2010; Çaydaş and Ekici 2012). Since waterjet grinding performance will be influenced by many unoptimizeable factors and interference signals, which weaken the reliability of process optimization with traditional simulations, ANFIS can deal with this difficult problem with better efficiency and higher accuracy (Tangwarodomnukun et al. 2014).

ANFIS uses a given data set of input and output variables to build up a fuzzy reasoning system. The combination of input and output proposes a series of positive causal relationships described by logic rules. In this paper, selection of input/output values should be able to demonstrate the working parameters of strengthen waterjet grinding, and then the resultant topography characteristics of ring surface. Therefore the input/output parameters were sampled according to their possible value ranges, and agglomerate concentration in actual machining condition simultaneously (Odior 2013; Akhavan Niaki et al. 2016; Abdulshahed et al. 2015a). With

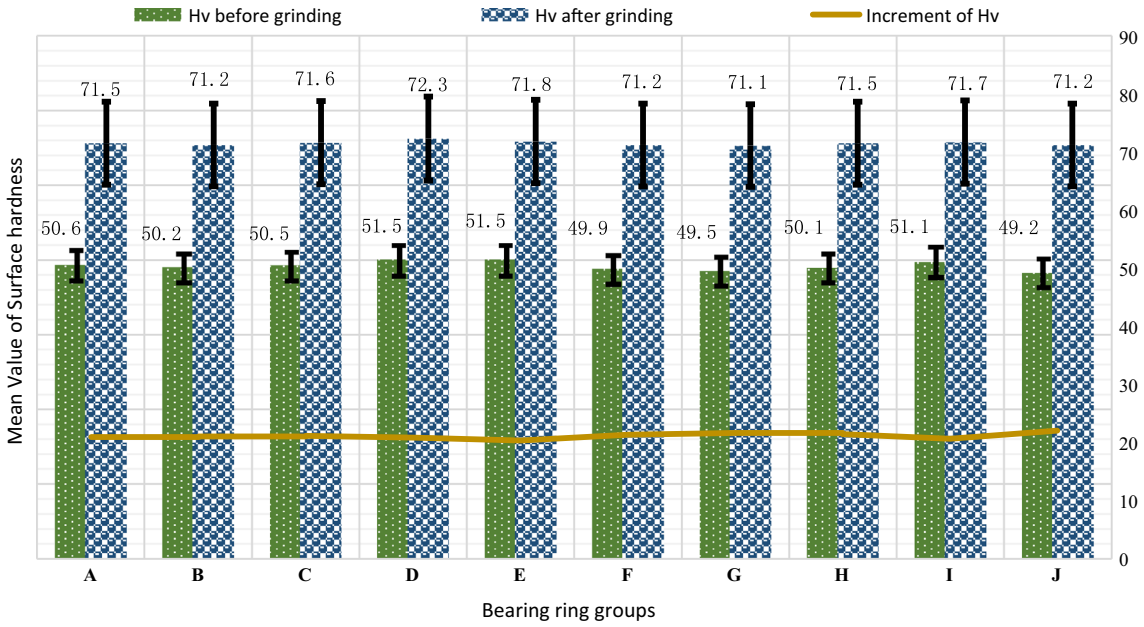

Fig. 6 H_v (HRC) of bearing ring before and after strengthen waterjet grinding grouped from A to J, as the mean values obtained from 12 measure points were exampled

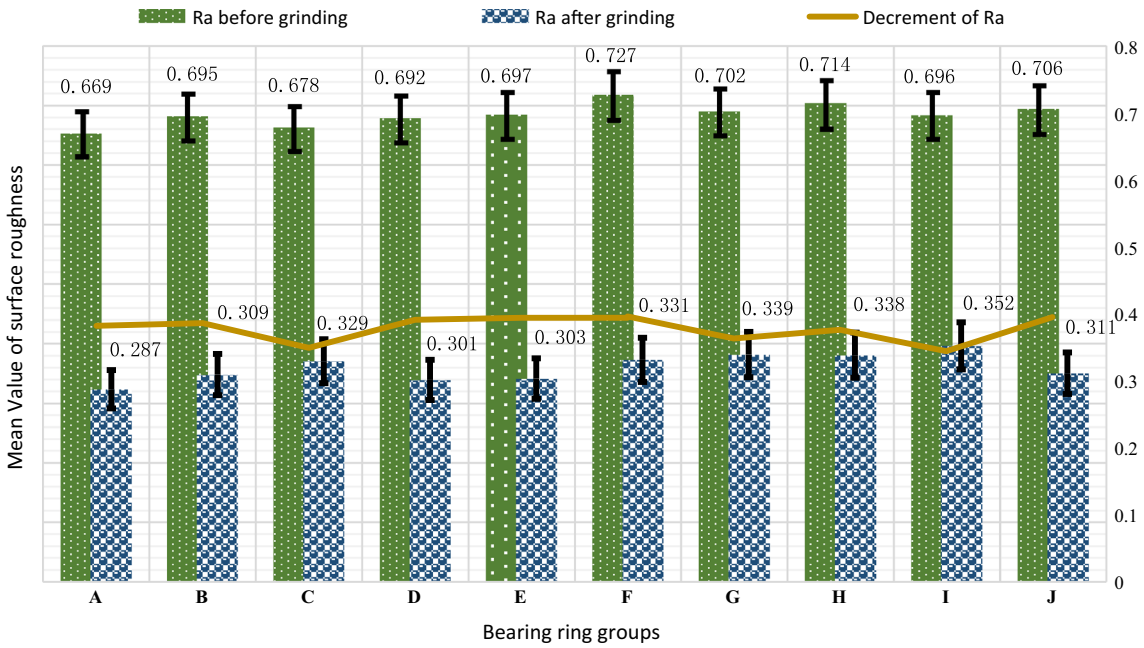

Fig. 7 R_a (um) of bearing ring before and after strengthen waterjet grinding grouped from A to J

the representative input/output values their mutual quantitative relations and complicated influence mechanism can be described clearly, the maximum reliability of input/output determination for ANFIS system can be achieved also.

To establish a reliable ANFIS system, more calculation elements (including nodes, weights, training data pairs, inputs, …, and so on) introduced, more accurate the ANFIS model setting and theoretical computation would be, accordingly the calculation time for ANFIS optimization would be lengthened exponentially also. Considering the existing limitation of workstation computing power, the reliability and sensitivity of ANFIS parameter setting should be verified in advance to ensure the stability of computation process and to determine its selection criterion. As Table 3 shows, seven typical setting schemes of ANFIS parameter were proposed, then the distribution variance, convergence time and conver-

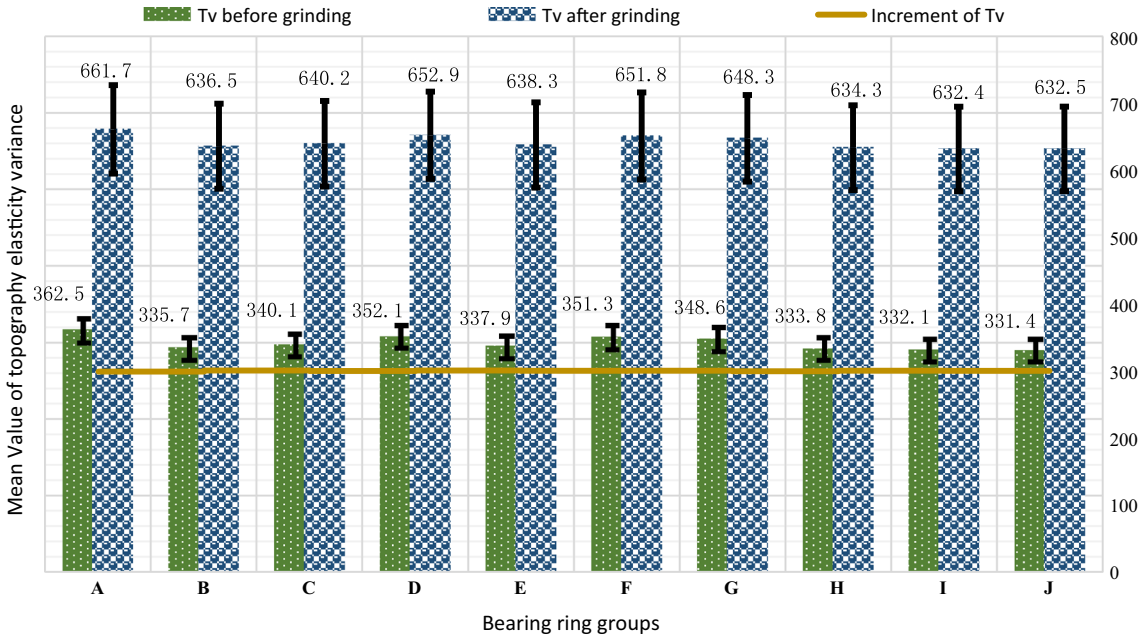

Fig. 8 T_v of bearing ring before and after strengthen waterjet grinding grouped from A to J

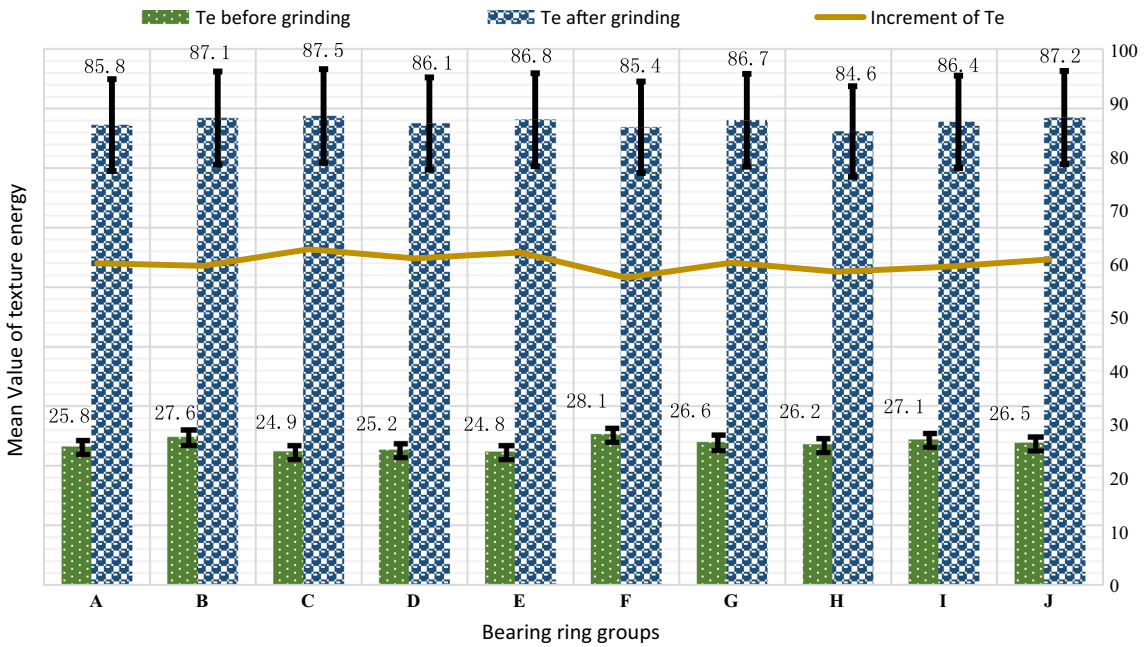

Fig. 9 T_e of bearing ring before and after strengthen waterjet grinding grouped from A to J

gence steps of H_v, R_a, T_v, T_e and L_d in circular calculations were focused on as the criterion for ANFIS information determination, and then compared to each other in an identical working condition, therefore an optimal scheme setting can be acquired. As demonstrated by Table 4, they all kept in a relatively low level from scheme I to III, and obtaining the lowest value by scheme III, which describes that the ANFIS optimized results on this stage keep stable and protect the computation model from the negative influences caused by parameter variation. On the other hand, the distribution variance, convergence time and steps of H_v, R_a, T_v, T_e and L_d changed significantly when other schemes being experimented, which reveals that the ANFIS computation process be more sensitive to parameter changing or environmental alternation in these conditions, detrimental to its accuracy and reliability particularly. Combined with actual

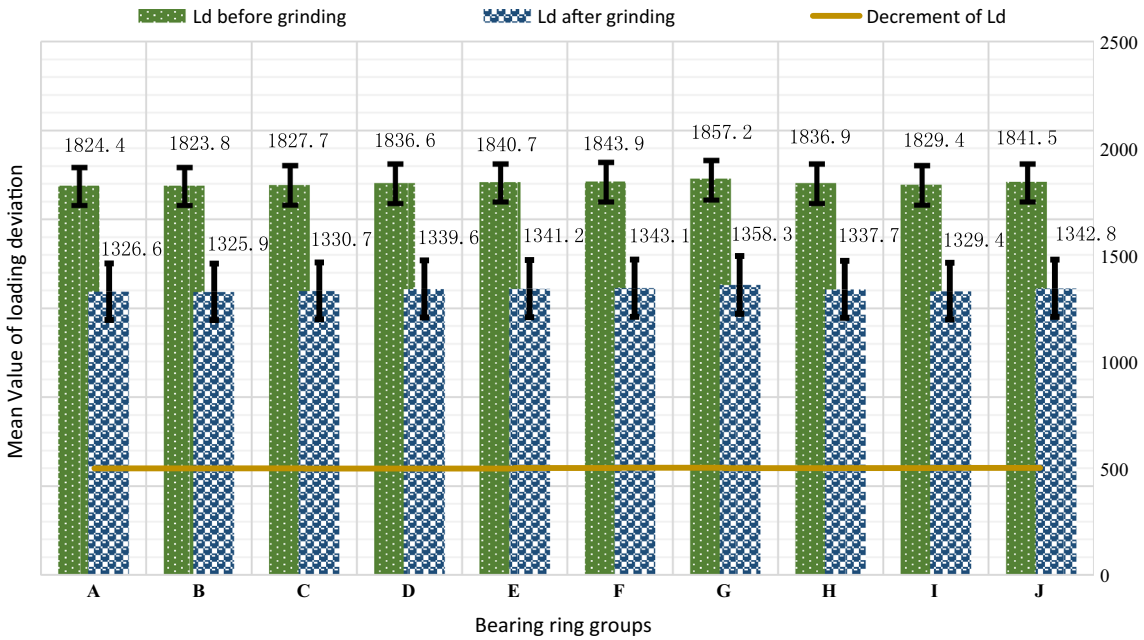

Fig. 10 L_d of bearing ring before and after strengthen waterjet grinding grouped from A to J

Table 3 Experimental schemes of ANFIS parameter setting

Setting scheme	I	II	III	IV	V	VI	VII
No. of nodes	85, 568	76, 244	65, 578	58, 668	56, 992	50, 048	48, 226
No. of linear weights	47, 726	38, 668	35, 488	34, 224	32, 226	30, 268	28, 868
No. of nonlinear weights	26, 448	25, 482	20, 090	19, 478	18, 668	17, 886	16, 482
No. of inputs	752	682	625	582	486	368	324
No. of training data pairs	780	726	680	556	534	426	388
No. of checking data pairs	780	682	660	624	582	546	498
No. of fuzzy rules	12, 600	11, 200	10, 000	9200	8000	7600	6000
Epochs for ANFIS training	2800	2600	2400	2200	2040	1860	1600

Table 4 The reliability and sensitivity verification for ANFIS parameter setting

Evaluation criterion		Setting scheme						
		I	II	**III**	IV	V	VI	VII
H_v	Distribution variance	23.22	16.15	**11.08**	22.75	14.65	14.61	14.21
R_a		22.59	17.58	**12.14**	23.05	13.47	15.18	16.28
T_v		25.33	19.22	**13.14**	18.75	15.02	16.28	19.84
T_e		24.11	18.47	**10.22**	16.22	17.00	17.71	20.14
L_d		24.15	16.66	**12.09**	14.17	14.86	15.09	15.35
H_v	Convergence time	0.55	0.41	**0.34**	0.25	0.44	0.62	0.72
R_a		0.48	0.42	**0.28**	0.36	0.41	0.45	0.58
T_v		0.68	0.53	**0.33**	0.42	0.51	0.55	0.82
T_e		0.77	0.61	**0.34**	0.47	0.47	0.57	0.87
L_d		0.69	0.67	**0.38**	0.48	0.57	0.69	0.88
H_v	Convergence steps	552	538	**361**	447	586	669	805
R_a		705	518	**343**	462	586	833	1129
T_v		664	498	**354**	447	516	548	865
T_e		629	522	**298**	452	487	511	872
L_d		526	455	**318**	526	459	596	767

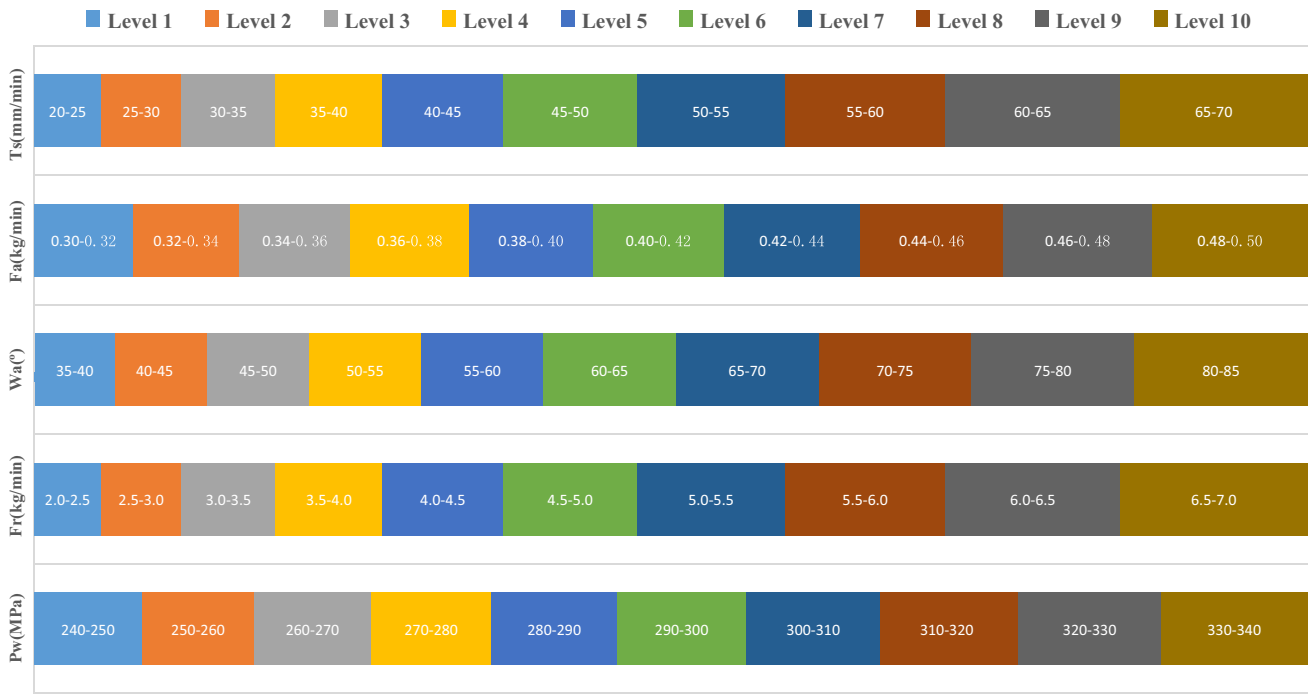

Fig. 11 The recommended levels of working parameters

experimental machining process, all the above-mentioned verification and determination criterion prove that scheme III, as highlighted in bold fonts, greatly contributes to parameter optimization and data analysis of ANFIS system, thus a more stable and accurate calculation can be realized.

Based on these steps, Fig. 11 presents the recommended levels of working parameters (P_w F_r W_a F_a T_s) as input, and Fig. 12 proposes the partitioned universes of the measure indexes ($H_v R_a T_v T_e L_d$) as output. The input and output universes should be partitioned into the range of (0–10), according to the minimum and maximum value allowed for ANFIS definition, with any value outside assumed to be infinity or zero (Muhammad et al. 2013). Figure 13 gives a representative arrangement of membership functions for R_a.

During the process of strengthen waterjet grinding, there are many factors influencing machining qualities, in which the working parameters stands up for key influence factors. Furthermore, it is the non-linear coupling relation between working parameters that determines the machining qualities and performance effect, so that the influence mechanism should be considered.

In order to quantify the non-linear coupling relations between waterjet working parameters, and investigate the operation mechanism of parameter combinations by ANFIS computation, the concept of orthogonal experiment design was introduced into the formation of fuzzy logic rules, since it presents a mathematical tool to study the influences by working parameters on the measure indexes of surface machined. Through studying the priority order of different working parameters, and determining the complicated correlations between parameter combinations and grinding performances, the optimal values for working parameters can be obtained after variance range analysis.

Orthogonal experiment design proposes a reliable foundation to establish ANFIS logic rules. As the number of working parameter combinations is often so large that it is impractical to test all computation experiments, which provides the best combination of participant parameter levels by drawing representative samples. Thanks to the parameter levels characterized by uniform distribution and mutual comparable, the number of ANFIS logic rules and experimental tests can be decreased significantly, which offering a simplified combination of factor levels for practical working analysis, and deleting the grinding defects on objective ring surface, therefore the orthogonal- experiment-design-based ANFIS logic rule benefits the improvement of strengthen grinding quality undoubtedly.

Orthogonal experiment works on an orthogonal array (OA) and factor analysis (FA) method. An OA with N factors and Q levels per factor was denoted by $L_M(Q^N)$, where L denotes the orthogonal array and M gives the number of experiment combinations. To establish OA several arrangement principles should be followed: Firstly, those important elements paying remarkable influences on orthogonal factors should be selected carefully, excluding the uncontrollable or negligible ones; Secondly, the influence factors should be arranged appropriately, their changing ranges or variance

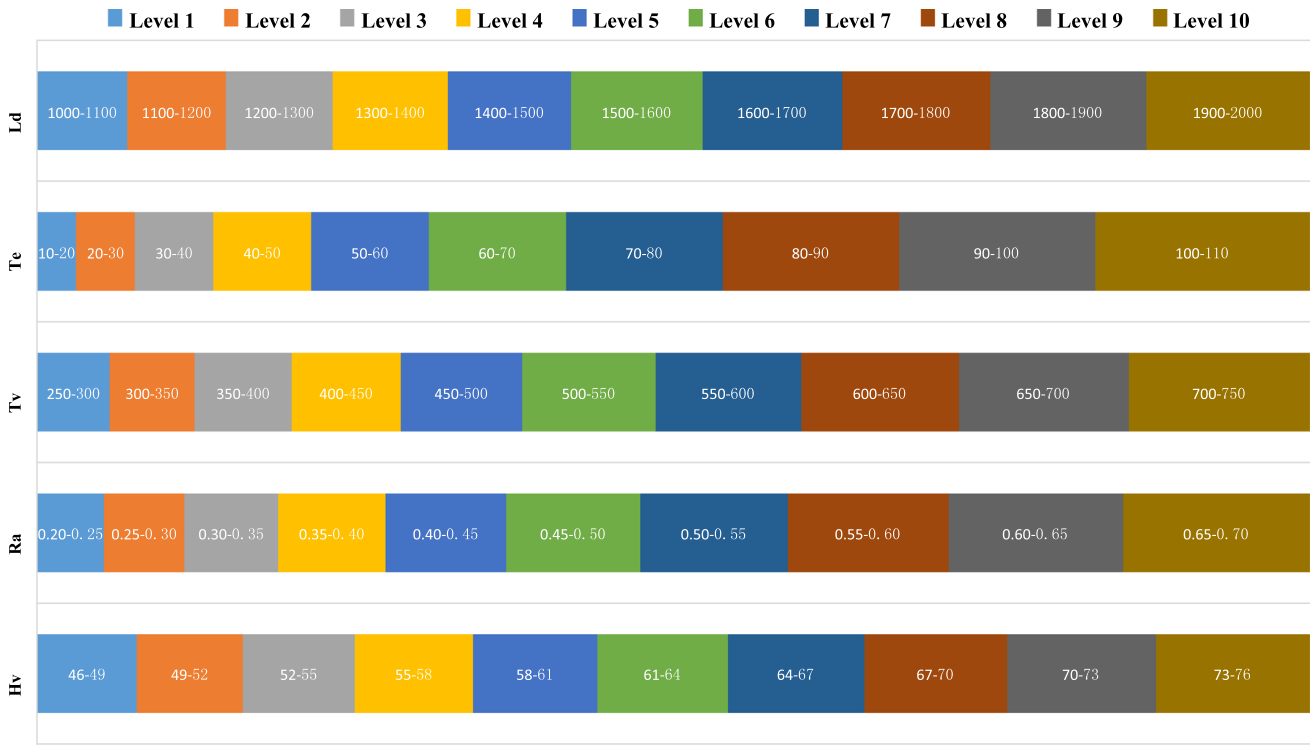

Fig. 12 The recommended ranges for the partitioned universes of the measure indexes

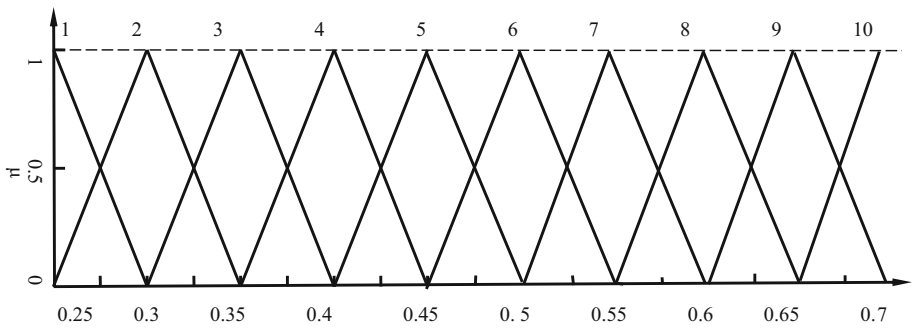

Fig. 13 A representative arrangement of membership functions for R_a (um)

levels should be identified according to practical machining capabilities or experimental condition, and homogenized-distributed in the whole universe of their possible values. Thirdly, the number of OA column keeps larger than that of influence factors. Based on these preconditions for factor settling and interaction determining, a relatively-small OA can be obtained to decrease experiment times or data pairs at the most extent. Finally, the freedom degree of OA keeps higher than that of factor, interaction, and error freedoms in total, the main effect of OA should be kept away from the significant interference caused by factor interactions.

Following steps were employed to establish fuzzy logic rules: Determining the experiment objective (the optimal working parameters for waterjet grinding) and establishing the target function (the ANFIS optimization function); Selecting the experimental indexes for ANFIS optimization (the measure indexes of ring surface grinded); Arranging the appropriate value levels for objective indexes; Making a suitable orthogonal combination array; Analysis of ANFIS optimization or orthogonal experiments; Calculating the optimal parameter combination for actual performance. Since the huge amount of full rule combinations can not be tested in ordinary condition, Table 5 gives the fuzzy logic rules according to orthogonal experiment arrangement, with the working parameters scattered uniformly over the space of all possible value combinations. For the purpose of clearly enunciating the logic rules of ANFIS operation, MATLAB's ANFIS editor offers typical types of membership functions for selection, including triangular, parabolic, Gaussian, Bell, Sigmoid, and trapezoidal-shaped functions, they were evaluated in precision and reliability sequentially, and thereafter triangular-shape membership function outperformed other

Table 5 Description of the orthogonal-experiment-design-based fuzzy logic rules for ANFIS system

No	Exp. run of input levels					Exp. run of output levels				
	P_w	F_r	W_a	F_a	T_s	H_v	R_a	T_v	T_e	L_d
1	1	1	1	1	1	4	5	2	1	9
2	1	1	2	1	3	5	3	6	5	5
3	1	2	3	1	5	6	3	7	4	2
4	1	2	4	2	9	8	8	8	7	8
5	2	3	5	2	10	7	7	1	9	5
6	2	3	6	2	2	10	1	5	5	6
7	2	4	7	3	7	5	2	1	1	2
8	2	4	8	3	8	6	4	2	2	4
9	3	5	9	3	6	2	8	4	6	10
10	3	5	10	4	4	4	9	4	10	4
11	3	6	1	4	2	8	10	7	4	8
12	3	6	2	4	5	1	2	5	1	5
13	4	7	3	5	7	3	5	2	8	9
14	4	7	4	5	1	5	7	6	2	1
15	4	8	5	5	3	4	4	2	6	4
16	4	8	6	6	10	1	3	7	3	5
17	5	9	7	6	8	2	6	5	5	6
18	5	9	8	6	9	2	8	2	4	10
19	5	10	9	7	6	5	10	4	7	8
20	5	10	10	7	4	8	4	8	5	4
21	6	1	1	7	3	6	2	9	9	2
22	6	1	2	8	8	9	5	10	5	2
23	6	2	3	8	7	8	9	5	6	5
24	6	2	4	8	2	10	1	10	3	8
25	7	3	5	9	1	5	1	4	8	6
26	7	3	6	9	5	4	2	8	4	10
27	7	4	7	9	9	7	2	1	1	7
28	7	4	8	10	10	2	3	10	5	5
29	8	5	9	10	6	2	4	3	6	3
30	8	5	10	10	4	6	8	5	2	5
31	8	6	1	9	8	5	6	2	8	8
32	8	6	2	9	6	5	4	6	9	6
33	9	7	3	9	4	8	8	7	4	4
34	9	7	4	8	3	7	2	9	6	3
35	9	8	5	8	2	3	7	2	5	5
36	9	8	6	8	5	2	6	4	5	8
37	10	9	7	7	9	4	2	7	6	10
38	10	9	8	7	1	5	6	3	7	2
…	…					…				
100	10	10	10	6	7	2	2	2	5	2

counterparts and yielded the best results. Amount of membership functions was chosen based on the number of input variables, since they should be kept fewer than the number of training data pairs. To make sure that the initial combination of input variables do not influence on the final optimized results, more than 80% of the inputs were selected for training while tenfold cross validation was conducted in ANFIS learning, both the training and testing sets should be uniformly sampled according to the orthogonal experiment table. Thanks to all these presupposed arrangements, ANFIS architecture can be formed by using five network layers and a set of orthogonal-experiment- design-based rules (Sarkheyli et al. 2015). Figure 14 illustrates the predetermined fuzzy logic rules of ANFIS system realized by Matlab, and Fig. 15 presents the ANFIS architecture used in this research, with its input and output variables outlined.

Part II: Application of ANFIS for grinding parameter optimization

Application of ANFIS optimization

As the ANFIS system discussed by this paper, it was the training and testing strategies that distinguish it from other alternatives. In ANFIS setting, the gradient-based learning algorithm was compared with other typical leaning algorithms in reasoning performance and calculation precision, such as Hybird Algorithm, Maximum Likelihood Method, Genetic Algorithm, Least Square Method, and Particle Swarm Optimization. After experimental running and data analysis, it was found that the gradient-based learning algorithm was characterized by simpler logic structure, fewer setting parameters, more reliable calculation performance, more effective process optimization, stronger searching capability, rapider convergence speed, and enjoys a profound background of intelligent control. This proposed learning algorithm can distinguish different input variables and initialize fuzzy logic rules automatically by its own fuzzy identification system, so that the membership functions, network weights and construction parameters can be adjusted adaptively.

A neuron in the orthogonal-experiment-design-based ANFIS network produces its output by processing the net input through nonlinear activation (transfer) function. As sigmoidal activate function was the most frequently utilized one, which updates the weight and derivative values of ANFIS according to resilient back propagation algorithm; therefore, it was usually trained for updating ANFIS networks, with the minimum Mean Square Error (MSE) between the calculation results caused by the network output and input variables of targeted neuron, were predetermined as the ultimate training objective.

With this training operation, the updated weight for ANFIS increases whenever the derivative value of its performance function has the same sign for two successive calculate iterations; on the other hand it decreases according to the derivative value with respect to that weight changes sign from

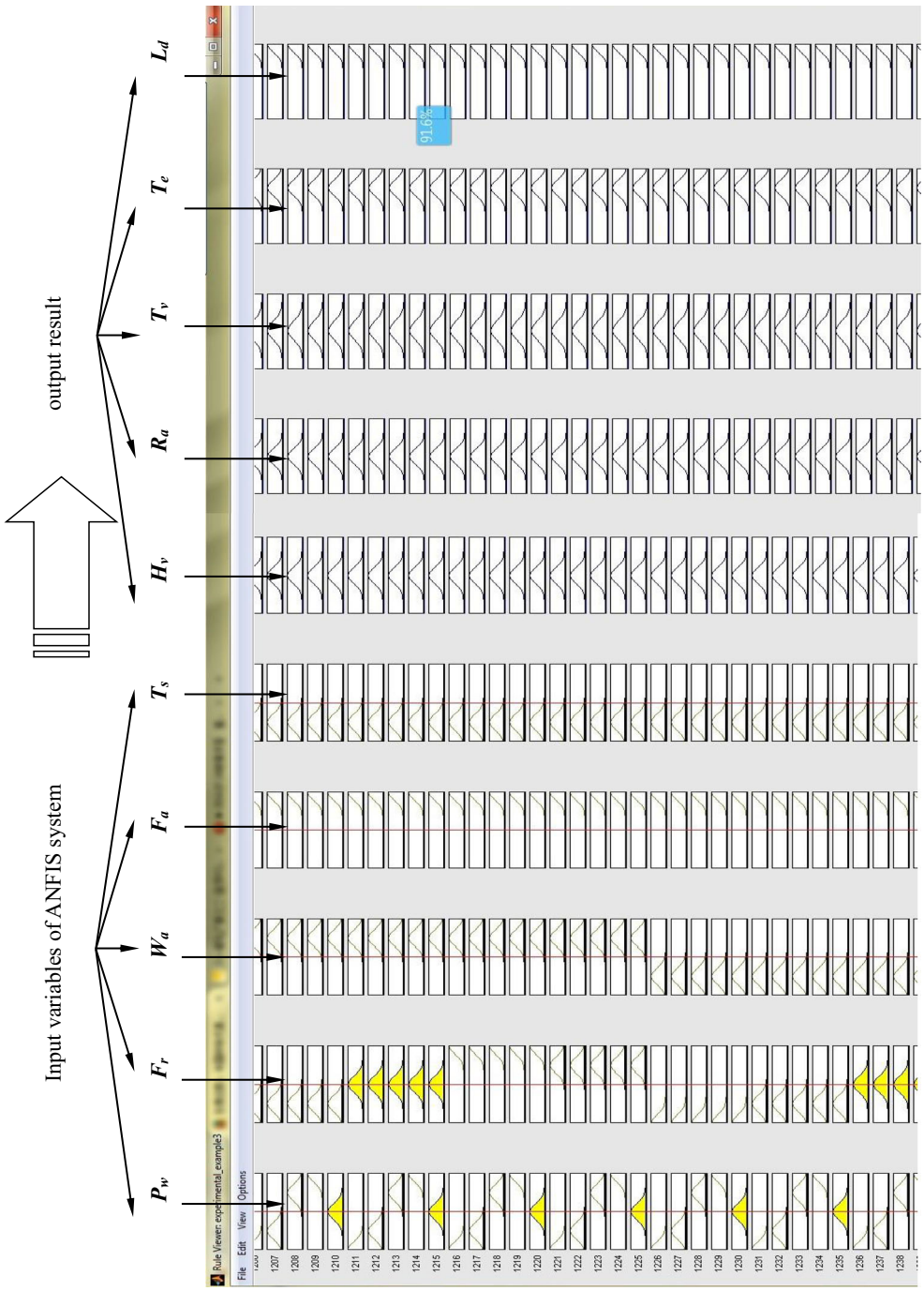

Fig. 14 The predetermined fuzzy logic rules of ANFIS system realized by Matlab

the previous iteration. If the derivative value keeps zero, the updated value for ANFIS weight remains the same; if the objective weight continues to change in the same direction for training iterations, the magnitude of weight change increases accordingly (Teimouri et al. 2015; Gajate et al. 2012).

When focusing on the ANFIS testing, it should be noted that the idea used for testing networks and applying test vectors was a multi-case test vector to determine the decision strength of this network. 300 data samples were prepared to describe the working parameters of strengthen waterjet grinding (Liang et al. 2012). Such a large testing case amount was employed to minimize the uncertainty of performance. Then, according to the membership functions of working parameters, they were inputted into the established ANFIS system and then check the obtained measure index results in sequence. The maximum possible reiteration times was

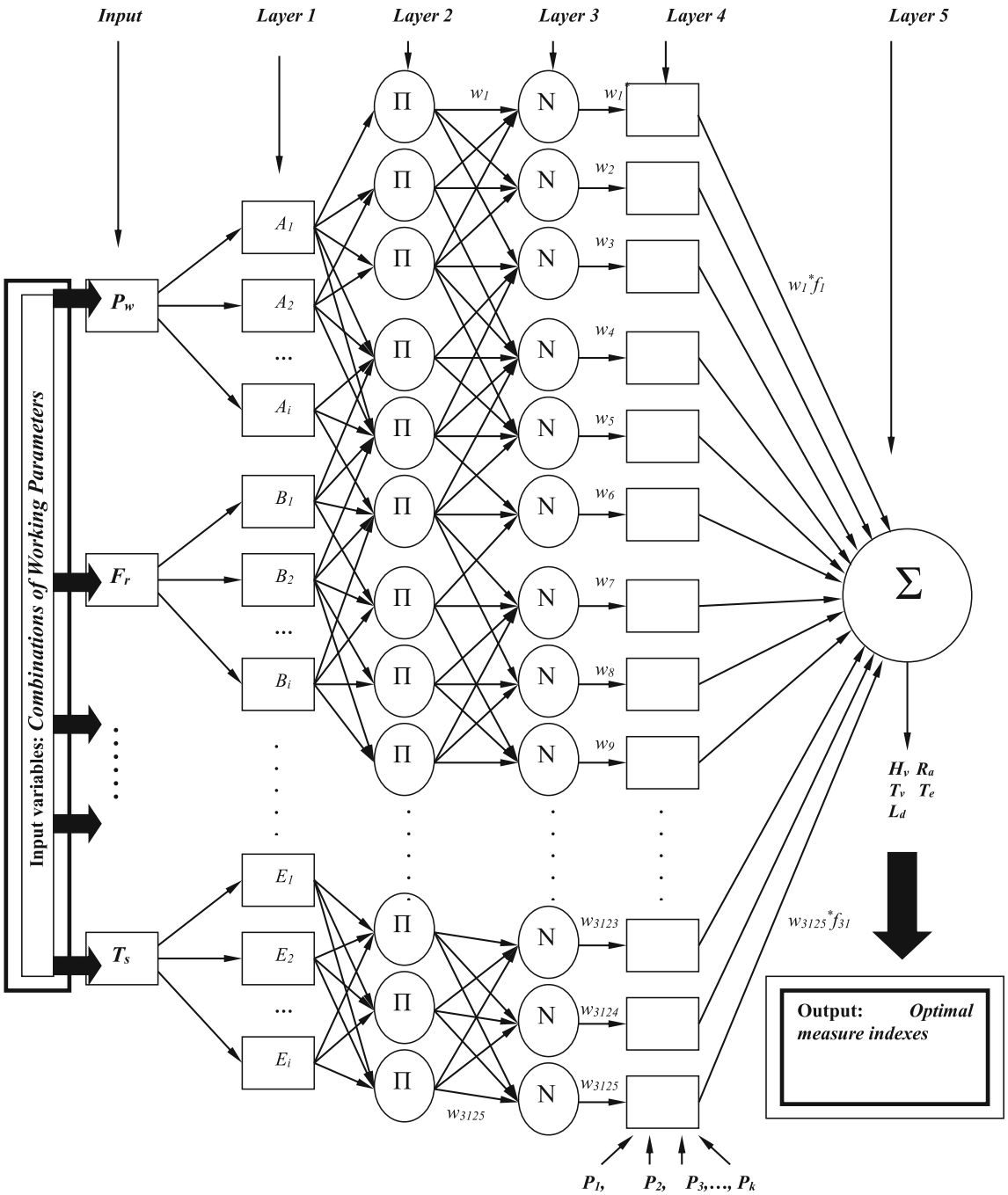

Fig. 15 ANFIS architecture used in this research, with its input and output variables outlined

17,000 to prevent the case of training threshold does not be met; the learning rate coefficient was supposed as 0.78, the momentum factor as 0.67, the training step as 1.36, and the interval illustration factor was predetermined as 50. Error function was defined to assess the ANFIS performance.

To evaluate the effectiveness of ANFIS, F-ratio-tests were applied to classify the total fluctuation of data into the part of the fluctuation caused by the change of influence factor (working parameter) level, and the remaining part caused by experimental error. Larger F-ratio value indicates that the influence factor, or working parameter, makes a greater impact on ANFIS performance. In addition, the contribution rate of working parameters was introduced to compare the relative importance of every parameter factor concerning with surface measure index Sevil Ergur and Oysal (2015).

The importance analysis of influence factors were shown in Tables 6, 7, 8, 9, and 10. Here, ** represents a highly significant factor; * denotes significant factor; and O means

Table 6 Importance analysis of factors for H_v

Influential factors	SS_e	Df_T	Q	F_j	Significance
P_w	65.25	8	1.875	14.15	**
F_r	7.22	8	0.358	2.11	O
W_a	39.25	8	1.511	18.47	**
F_a	18.14	8	0.698	9.87	*
T_s	39.77	8	1.475	16.55	**

Table 7 Importance analysis of factors for R_a

Influential factors	SS_e	Df_T	Q	F_j	Significance
P_w	48.78	8	2.577	17.78	**
F_r	36.55	8	2.389	16.89	**
W_a	12.14	8	1.844	5.24	*
F_a	5.15	8	0.784	2.11	O
T_s	3.66	8	0.644	3.18	O

Table 8 Importance analysis of factors for T_v

Influential factors	SS_e	Df_T	Q	F_j	Significance
P_w	15.74	8	1.925	8.26	*
F_r	14.22	8	1.875	7.14	*
W_a	36.88	8	5.478	18.14	**
F_a	16.34	8	1.648	6.89	*
T_s	6.59	8	0.598	2.34	O

Table 9 Importance analysis of factors for T_e

Influential factors	SS_e	Df_T	Q	F_j	Significance
P_w	36.54	8	2.879	19.45	**
F_r	10.25	8	1.548	8.47	*
W_a	12.47	8	1.722	7.48	*
F_a	16.22	8	1.324	9.65	*
T_s	40.21	8	2.265	18.78	**

Table 10 Importance analysis of factors for L_d

Influential factors	SS_e	Df_T	Q	F_j	Significance
P_w	6.55	8	0.547	3.68	O
F_r	18.47	8	1.226	9.22	*
W_a	40.21	8	3.654	21.44	**
F_a	36.47	8	2.568	18.47	**
T_s	17.26	8	1.482	10.25	*

no impact. As can be seen that the effects of P_w, W_a and T_s on surface hardness are remarkable; P_w and F_r have greater impact on surface roughness than other alternatives. Simultaneously, the influence caused by W_a on elasticity

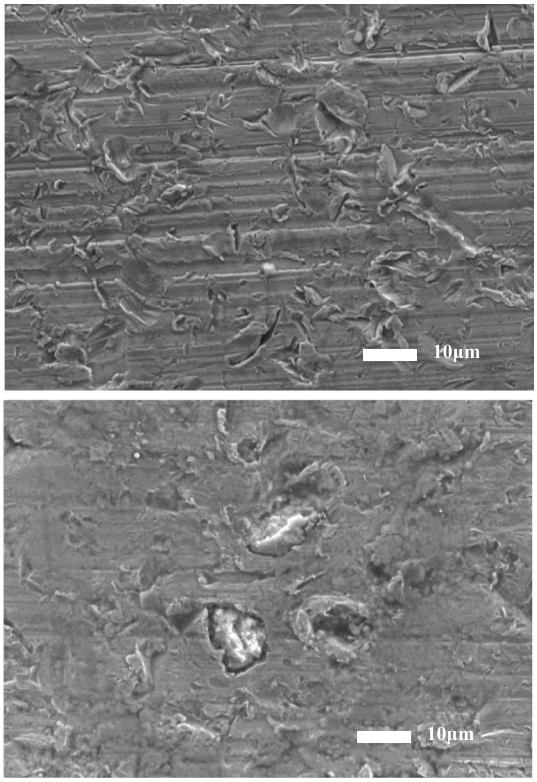

Fig. 16 Representative performance effectiveness by using two working parameter groups

variance cannot be ignored. Further analysis shows that P_w and T_s were the most powerful influence factors for texture energy, while W_a or F_a become crucial for topography loading deviation. After identifying the influences caused by waterjet working parameters, the optimized results of ANFIS system can be controlled through verifying the correspondingly influence factors. Figure 16 presents the representative performance effectiveness of waterjet grinding on bearing ring surface, by using two working parameter groups. Figure 17 illustrates the grinding performances by using the ANFIS-optimized working parameters, from which the result improvements can be observed more closely.

Optimization results and performance discussions

Figures 18, 19, 20, 21, and 22 present the result improvements of grinded surface between using and not using the ANFIS- optimized working parameters, as the influences caused by P_w, F_r, W_a, F_a, and T_s were emphasized in sequence. In these figures, red column demonstrates the optimized working parameters, while the original ones without ANFIS optimization were highlighted in blue. Horizontal axes denote the targeted measure indexes of ring surface topography under the influences of working parameters (or

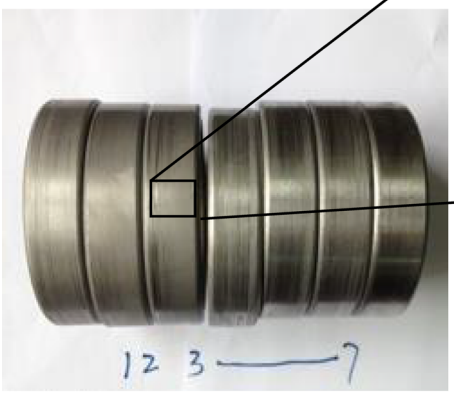

Objective bearing rings to be machined

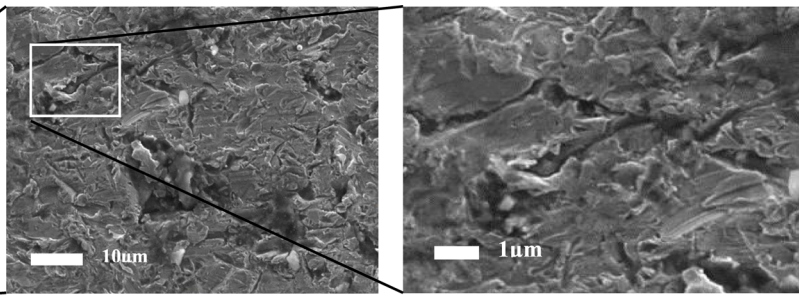

The electro-microscope of ring surface before strengthen waterjet grinding

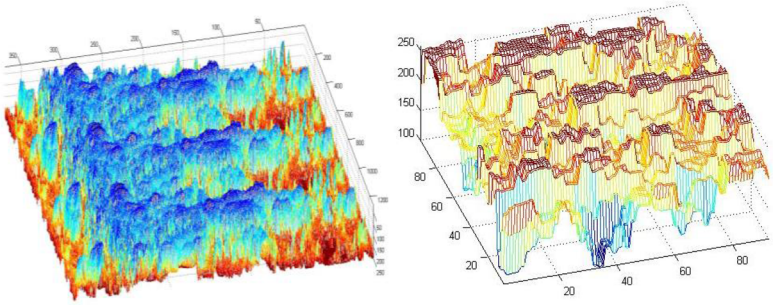

The reconstructed surface topography model of original surface

Stage 1: Topography details on bearing ring surface before strengthen waterjet grinding

Obtained bearing rings after strengthen waterjet grinding

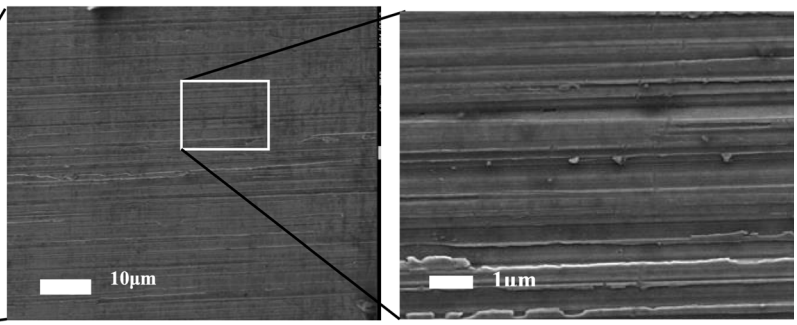

The electro-microscope of grinded surface by using the ANFIS-optimized working parameters

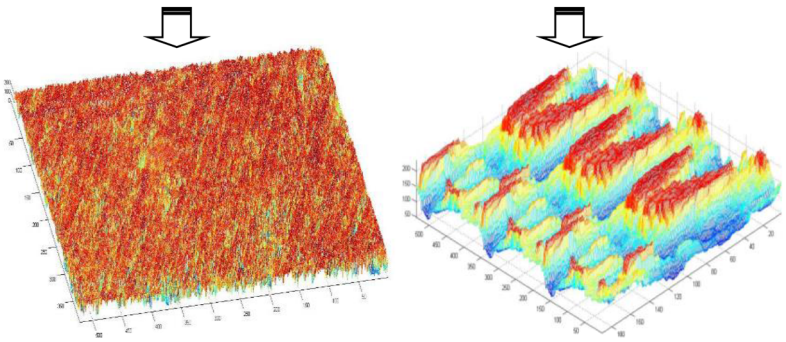

The reconstructed surface topography model of surface grinded

Stage 2: Performance effectiveness of strengthen waterjet grinding on bearing ring surface by using the ANFIS-optimized working parameters

Fig. 17 Performance of strengthen waterjet grinding on bearing ring surface by using the ANFIS-optimized working parameters

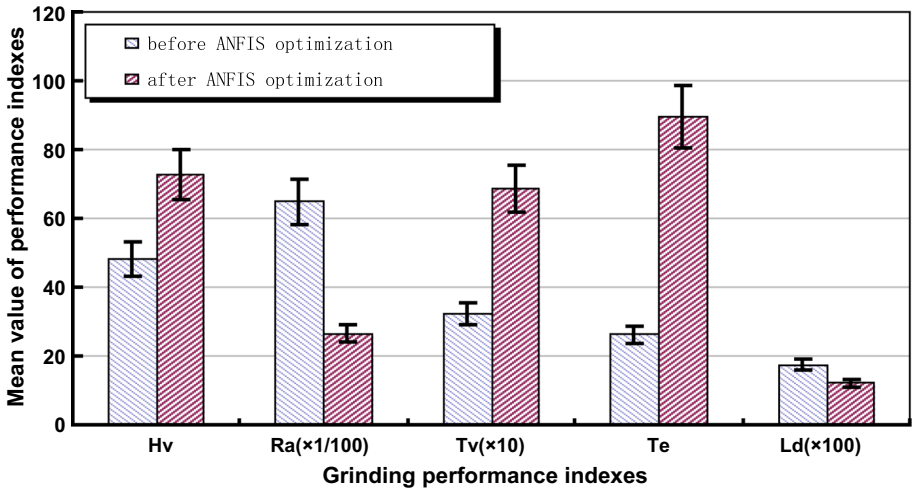

Fig. 18 Result improvements between using and not using the ANFIS-optimized working parameters, considering the influences caused by P_w

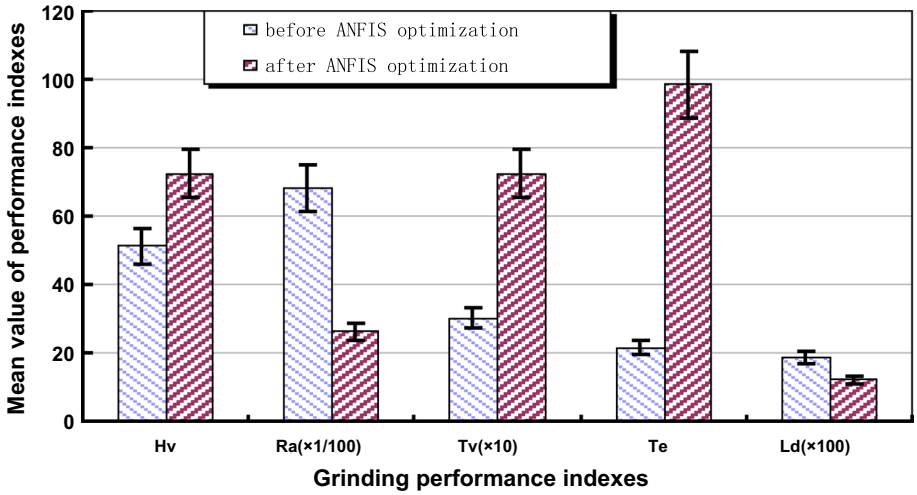

Fig. 19 Result improvements between using and not using the ANFIS-optimized working parameters, considering the influences caused by F_r

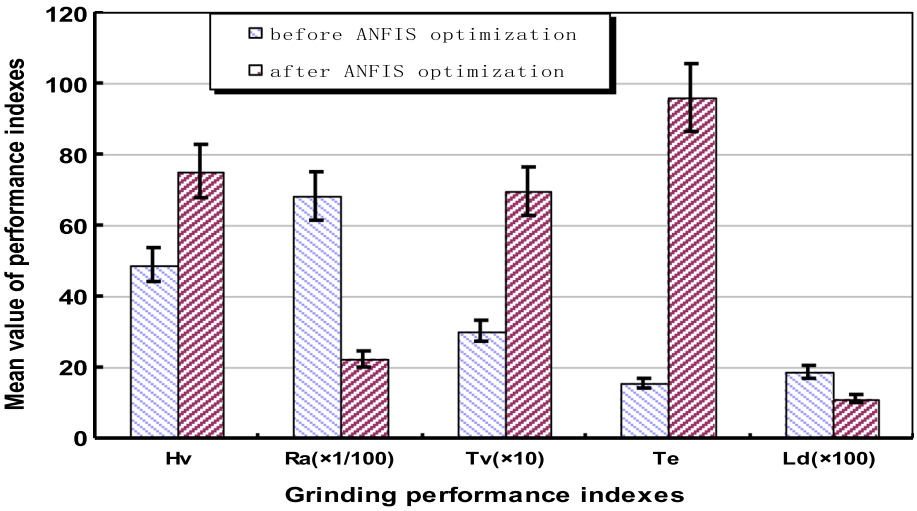

Fig. 20 Result improvements between using and not using the ANFIS-optimized working parameters, considering the influences caused by W_a

called as the grinding performance indexes), while vertical axes show the result comparisons with and without ANFIS optimization accordingly, as the mean values of measure indexes were employed. It can be learned from them that the optimized working parameters result to remarkable quality improvements on surface topography compared to those original ones, though some deviations exist because of noise data or truncate error caused from ANFIS calculation Liang

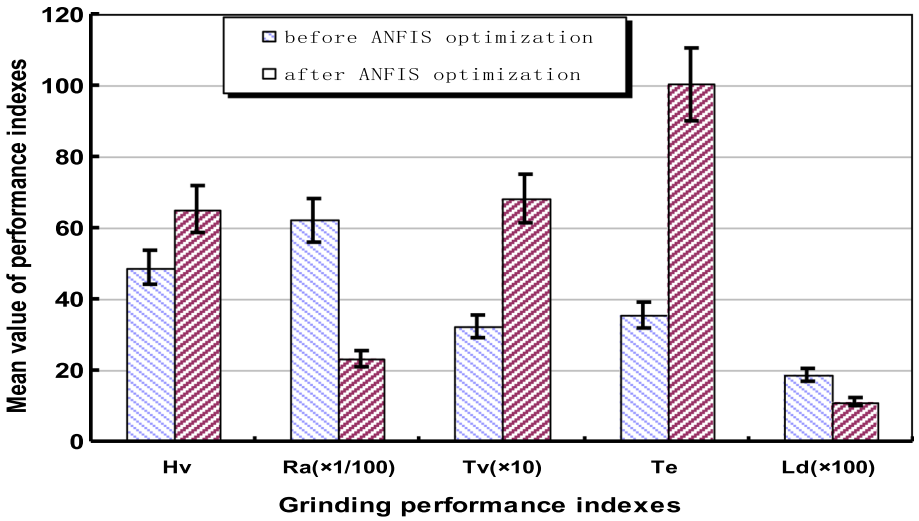

Fig. 21 Result improvements between using and not using the ANFIS-optimized working parameters, considering the influences caused by F_a

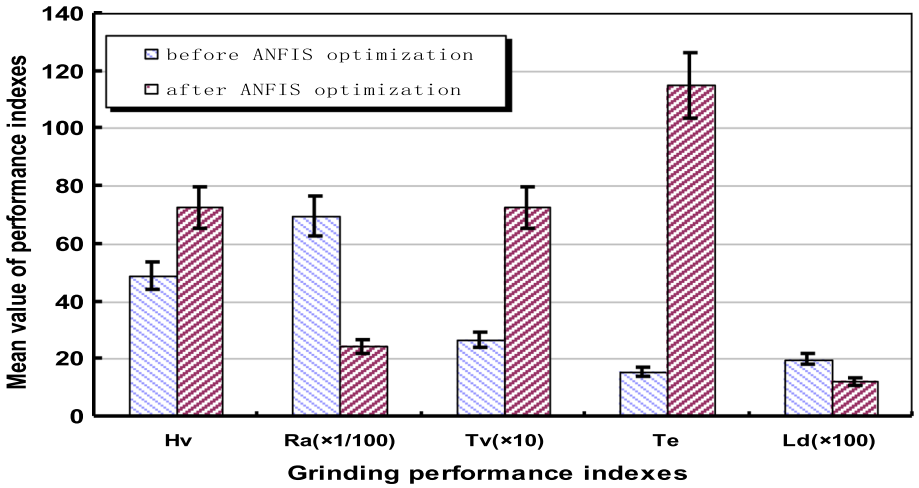

Fig. 22 Result improvements between using and not using the ANFIS-optimized working parameters, considering the influences caused by T_s

et al. (2015). In this work, ANFIS optimizations of working parameter depend on the past observations for times using the historical measurements of surface measure indexes on different ring specimens Liang et al. (2012). In this sense, optimization process was linked to the fuzzy logic environment and the innovative architecture of ANFIS, providing a better performance over other traditional works.

With Fig. 18 and Table 6 it can be obviously seen that surface hardness was remarkably influenced by P_w. And it was also easily impacted by W_a and T_s. Surface hardness describes the inherent capabilities of grinded surface to resist external waterjet impact force, thereafter T_s becomes a basic theoretical foundation for grinding stress control, especially for topography elasticity variance or texture energy. This figure shows that surface hardness caused by the optimized working parameters keeps higher than that of other alternative samples. Moreover, texture energy reaches an optimal state, which explains the wide applications of F_r in a preliminary hardness increment or material characteristic improvement of waterjet semi- finishing processes, especially when the layer metallographic variances of ring surface were fully considered about (Liang et al. 2016).

Surface roughness (Fig. 19; Table 7) obviously keeps a considerable close correlation with P_w or F_r, it also highly dependents upon W_a in practical operation. Due to the proposed ANFIS system gives a reference index for surface roughness, its variation causes a correspondingly fluctuation in texture unit density. The proposed ANFIS system can be fully employed to promulgate the distribution rationality of loading deviation and texture energy. Result comparison of roughness values on ring samples demonstrates that with the application of ANFIS optimization, surface roughness keeps a remarkably decreasing state, showing that ANFIS optimization plays an important role in the equilibrium distribution of surface roughness, and contributes to a more stable grinding performance on ring surface as respected.

Topography elasticity variance (Fig. 20; Table 8) markedly affected by W_a and keeps a close correlation with P_w or

F_r, which shows the probability and feasibility of transforming surface shape and elasticity stress distribution by considering impacting loading or work-hardening capacities. This figure shows that, although performance improvements were realized in elasticity variance, the ANFIS-optimized one still keeps in a more stable state, provides a useful tool to markedly eliminate elasticity loading interference (Liang et al. 2014); simultaneously, it also ensures a much better grinding effectiveness, and maintains stable loading deviation when the self-adaptive synchronous grinding employed. Elasticity variance was usually used for calibrating the obtained ring surface under the influences of residual stress distribution.

Texture energy (Fig. 21; Table 9) was obviously influenced by P_w or T_s. It also highly dependent upon W_a, together with F_a being considered. It was learned that the optimized parameters present a more equally distribution of grinding allowances when severe conditions happened. Result comparisons demonstrate that although texture energy improvements were realized, machining accuracy and texture density still kept in an unimproved situation, showing that the optimal flatness degree or surface plainness can not be easily ensured, unless effective optimization were accompanied with (Nguyen et al. 2008). Parameter optimization neglects some kinds of machining errors or grinding defects such as transitional stepping and concentrated wearing, which explains its currently wide application in the finished shape calibration, especially when the force interference emerged, or the residual stresses of bearing ring surfaces were paid high attention to.

Loading deviation (Fig. 22; Table 10) keeps a rather closely relation with W_a and F_a, it also partially determined by F_r and T_s. The ANFIS optimization of working parameters maintains better machining quality and stable finishing precision on curvature tolerance or machining accuracy, according to the above-mentioned process illustrations. The loading deviation in finished surface keeps a relatively superior performance; consequently, it improves the precision and accuracy of surface topography (Teimouri and Baseri 2015). When faced with interferential machining conditions, this optimization method provides a useful process feedback or standard check index to present an optimal parameter group. It also can be learned that the manufacturing performance and surface quality highly depend upon surface hardness and roughness, with a high-level parameter or diminished forming error were strongly recommended for, so that loading deviation and texture energy can be improved obviously.

In order to compare this new approach with other alternative ones, several typical parameter selection methods were testified, including Genetic parameter optimization, SA–GA (Simulated Annealing-Genetic Algorithm) parametric prediction, Taguchi parameter estimation, ANN–SA (Artificial Neural Network-Simulated Annealing) parametric selection, and GONNs (Genetically Optimized Neural Network Systems) parameter selection as well. It is noteworthy to point out that an identical machining condition proposed by "Establishment of experimental environment" section and Tables 1 and 2 was prepared, exampled by one complete surface-machining cycle for the outer ring of GCr15 deep groove ball bearing (DGBB) sized by 72.00 mm in diameter. The resultant grinding performances by using all these approaches were observed closely, then a detailed note can be taken about the measure indexes from the 1st to 10th machining cycles; thereafter, a statistical assessment on their average performances was conducted.

A set of Measure Level Index (MLI) returns the value level on which the measure index of surface topography situates. As the MLI of H_v value used as a representative example and shown as follows:

$$MLI(H_{\mathrm{v}}) = \frac{\sum_{m=1}^{k} m H_v(m)}{\sum_{m=1}^{k} H_v(m)}; m = 1, 2, \ldots, k \tag{4}$$

Average Relative Percent (ARP) of optimal measure index was proposed to assess actual working capabilities:

$$E_i(H_{\mathrm{v}}) = \left[\frac{(MLI(H_{\mathrm{v}}))_{\mathrm{or}i\mathrm{ginal},i} - (MLI(H_{\mathrm{v}}))_{\mathrm{optimal},i}}{(MLI(H_{\mathrm{v}}))_{original,i}} \times 100\% \right] \tag{5}$$

Here i represents the number of experimental samples. The ARP indexes of measure indexes by using different optimization algorithms can be illustrated in radar diagram as Fig. 23; Considering the fact that each algorithm has its own superiorities in different measure indexes, their performances can be evaluated and compared in the form of pentagon areas, as encircled by their ARP indexes in radar diagram axes:

$$\begin{aligned} &\text{Performance Improvement Index} = \mathrm{Are}a(P\mathrm{entagon_i}) \\ &= \frac{1}{2}\sin\frac{360^\circ}{5}[E_i(H_v)\cdot E_i(R_a) + E_i(T_v)\cdot E_i(R_a) \\ &+ E_i(T_v)\cdot E_i(T_e) + E_i(T_e)\cdot E_i(L_d) + E_i(L_d)E_i(H_v)] \end{aligned} \tag{6}$$

Comparing the pentagon areas resulted by different optimization methods, pentagon with the maximum area presents the most remarkable performance improvement in overall consideration, therefore an integrated performance evaluation of strengthen waterjet grinding can be obtained. Through working comparisons of performance improvement indexes, Genetic parametric optimization ensures a good performance

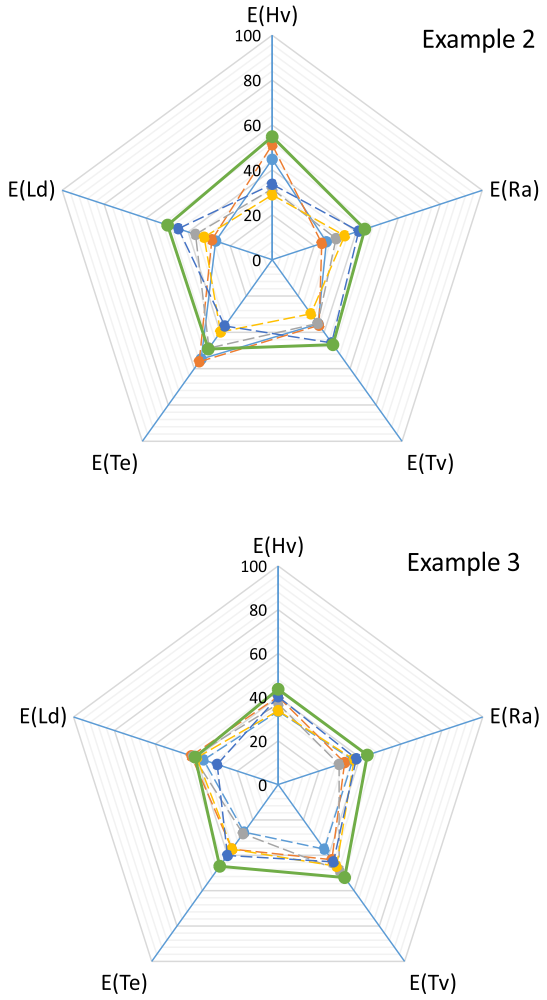

Fig. 23 Performance comparisons of different optimization methods by use of radar diagrams, as three representative examples selected out from 10 working conditions

in H_v and R_a, since it is more suitable to rapidly promote the effectiveness concentration of multi-phase waterjet flow on objective ring surface; SA–GA parametric prediction returns an excellent grinding performance when T_v to be highly emphasized on; ANN–SA parametric selection provides a remarkable improved result in T_e or T_v. Taguchi and GONNs methods have good capabilities in T_e and L_d, which deserve a more robust surface quality of waterjet grinding effectiveness in machining domain; Finally, Fig. 23 shows that the ARP indexes of ANFIS optimization outperforms other alternatives in pentagon areas, especially in R_a, T_v and L_d, demonstrating that ANFIS provides an optimal performance improvement in actual machining experiments. Its parametric optimization based on the assumption that the interaction between the given strengthen waterjet conditions and the concentration state of grinding effectiveness was an empirical—imprecise relationship. Performance comparison proves the validation and efficiency of this improved ANFIS-based parameter optimization method, therefore, its application and superiority can be verified accordingly.

Table 11 presents the statistical information of the optimal working parameters by ANFIS optimization, the machining processes and result comparisons indicate that:

* Higher level of P_w or F_r were necessary for increasing surface hardness, when those bearing-ring specimens processed with comparatively higher W_a and lower T_s;
* The optimal P_w for strengthen waterjet grinding is around 310 MPa, while the best value range for W_a should be limited into $60 - 75°$;
* When discussing the optimal T_s, about 85.3% surface quality improvements were obtained at about 60mm/min, the optimized F_r was about 5.8 kg/min, and F_a about 0.4 kg/min;
* Away from the optimal working parameters, actual performance of strengthen waterjet grinding was worse than that by using the ANFIS-optimized ones for normal ring machining, in an obviously way.

Following theoretical superiorities can be learned from this paper: As traditional studies did not touched upon the waterjet-machined qualities of bearing ring, a series of physical measure indexes were proposed to calibrate its surface topography; For the ordinary researches simply focused on waterjet grinding evaluation without any further considerations about the important impact caused by working parameters, this research tried to made comparisons between

Table 11 Statistical information of the optimal working parameter by ANFIS optimization

Working parameter	Optimal value	Standard error	Confidence interval of 95%	
			Upper limit	Lower limit
Waterjet pressure (P_w/MPa)	310	4.2	314.2	305.8
Flow rates of water mass (F_r/ kg/min)	5.8	0.12	5.92	5.68
Waterjet attack angle (W_a/°)	70	1.3	71.3	69.7
Mass rate of abrasive grit (F_a/kg/min)	0.4	0.07	0.47	0.33
Traverse speed (T_s/mm/min)	60	1.2	61.2	58.8

the waterjet grinding performance by using ordinary parameters, and that by using the ANFIS-optimized ones obtained from orthogonal experiment and miscellaneous data analysis; Different from traditional investigations concluding waterjet grinding effectiveness from a macro-scale data statistics or dynamic machining simulation, an improved ANFIS system based upon orthogonal experiment design, was proposed to optimize the working parameters of waterjet grinding, and to distinguish different influences of participant parameters on the ring surface machined; Therefore this research fulfilled the task of determining the optimal working parameters for strengthen waterjet grinding, with fewer experiment iterations compared to other alternative approaches. Final conclusions were obtained based on the theoretical investigations, and result comparisons between the strengthen waterjet grinding performances by employing the ANFIS-optimized working parameters and other ordinary ones.

Conclusions

This paper sought to optimize the working parameters of strengthen waterjet grinding with an orthogonal-experiment-design-based ANFIS system. Actual performance evaluation and working parameter optimization concerning with the measure indexes of bearing-ring surface, together with the application of ANFIS system, were the main focus of this research. It can be realized by establishing an applicable ANFIS system generated from fuzzy membership functions, orthogonal experiment combinations and fuzzy logic rules, thereafter this proposed system quantitatively evaluates and demonstrates the complicated interrelation among all participant influence factors in waterjet grinding effectiveness. Actual machined results obtained indicate that remarkable improvements in machining performance can be achieved by using this approach with an appropriate setting of working parameters. Comparison between waterjet grinding processes with and without ANFIS optimization greatly help to provide a useful theoretical basis for machining improvement in return, which explains its preferences on realizing grinding optimization and facilitating machining efficiency in practical experiments.

As future work the specific influence factors of strengthen waterjet grinding and their inherent interrelation mechanism will be investigated further, especially on other key working parameters and their optimal combination settings; Furthermore more kinds of abrasive grits, grinding enhanced liquid and their physicochemical influences on machining process are going to be studied, in the hope of assessing the actual working effectiveness simultaneously. Additionally, the quantitatively correlations between waterjet parameters and their resultant dynamic grinding processes will be observed also, for the purpose of providing more reliable data references for grinding monitory in practical industrial conditions.

Acknowledgements The author acknowledges the funding of following science foundations: the National Natural Science Foundation of China (51575116), the China National Spark Program (2015GA780065), the Innovative Academic Team Project of Guangzhou Education System (1201610013), the Science and Technology Planning Project of Guangdong Province (2016A010102022), the Science and Technology Planning Project of Guangzhou municipal government, the Water Resource Science and Technology Program of Guangdong Province of China (2012-11), the Postgraduate Education Innovation Program of Guangdong Province (2016XSLT24), The Foundation for Fostering the Scientific and Technical Innovation of Guangzhou University (GZHU[2016]-92), and The Key Integration Project of Industry, Education and Research of Guangzhou University were appreciated for supporting this work, the editors were thanked also for their hard work and the referees for their comments and valuable suggestions to improve this paper.

Compliance with ethical standards

Conflict of interest The author(s) declared no potential conflicts of interest with respect to the research, authorship and/or publication of this article.

References

Abdulshahed, A. M., Longstaff, A. P., & Fletcher, S. (2015a). The application of ANFIS prediction models for thermal error compensation on CNC machine tools. *Applied Soft Computing*, *27*(3), 158–168.

Abdulshahed, A. M., Longstaff, A. P., Fletcher, S., & Myers, A. (2015b). Thermal error modelling of machine tools based on ANFIS with fuzzy c-means clustering using a thermal imaging camera. *Applied Mathematical Modelling*, *39*(7), 1837–1852.

Abhishek, K., Panda, B. N., Datta, S., & Mahapatra, S. S. (2014). Comparing predictability of genetic programming and ANFIS on drilling performance modeling for GFRP composites. *Procedia Materials Science*, *6*(5), 544–550.

Al-Ghamdi, K., & Taylan, O. (2015). A comparative study on modelling material removal rate by ANFIS and polynomial methods in electrical discharge machining process. *Computers & Industrial Engineering*, *79*(4), 27–41.

Akhavan Niaki, F., Feng, L., Ulutan, D., & Mears, L. (2016). A wavelet-based data-driven modelling for tool wear assessment of difficult to machine materials. *International Journal of Mechatronics and Manufacturing Systems*, *9*(2), 97–121.

Axinte, D. A., Stepanian, J. P., Kong, M. C., & McGourlay, J. (2009). Abrasive waterjet turning–An efficient method to profile and dress grinding wheels. *International Journal of Machine Tools and Manufacture*, *49*(3–4), 351–356.

Azmi, A. I. (2015). Monitory of tool wear using measured machining forces and neuro-fuzzy modelling approaches during machining of GFRP composites. *Advances in Engineering Software*, *82*(3), 53–64.

Bilbao Guillerna, A., Axinte, D., & Billingham, J. (2015). The linear inverse problem in energy beam processing with an application to abrasive waterjet machining. *International Journal of Machine Tools and Manufacture*, *99*(4), 34–42.

Çaydaş, U., & Ekici, S. (2012). Support vector machines models for surface roughness prediction in CNC turning of AISI 304 austenitic stainless steel. *Journal of Intelligent Manufacturing*, *23*(3), 639–650.

Chen, S., & Jiang, Z. (2015). A force controlled grinding-milling technique for quartz-glass micromachining. *Journal of Materials Processing Technology*, *216*(4), 206–215.

Dong, L., Sun, Y. D., & Li, D. J. (2010). Optimal deposition and layer modulation parameters for mechanical property enhancement of TiB_2/Si_3N_4 multilayers using orthogonal experiment. *Surface and Coatings Technology*, *205*(1), S422–S425.

Fan, D., Ni, W., Yan, A., Wang, J., & Cui, W. (2015). Orthogonal experiments on direct reduction of carbon-bearing pellets of Bayer Red Mud. *International Journal of Iron and Steel Research*, *22*(8), 686–693.

Gajate, A., Haber, R., del Toro, R., Vega, P., & Bustillo, A. (2012). Tool wear monitoring using neuro-fuzzy techniques: A comparative study in a turning process. *Journal of Intelligent Manufacturing*, *23*(3), 869–882.

Gao, X., Zhang, Y., Zhang, H., & Qiong, W. (2012). Effects of machine tool configuration on its dynamics based on orthogonal experiment method. *Chinese Journal of Aeronautics*, *25*(2), 285–291.

Hayasi, M. T., & Asiabanpour, B. (2013). A new adaptive slicing approach for the fully dense freeform fabrication (FDFF) process. *Journal of Intelligent Manufacturing*, *24*(4), 683–694.

He, Z., Sun, Y., Zhang, G., Hong, Z., Xie, W., Xin, L., et al. (2015). Tribological performances of connecting rod and by using orthogonal experiment, regression method and response surface methodology. *Applied Soft Computing*, *29*(3), 436–449.

Jia, X., Guo, F., Huang, L., Salant, R. F., & Wang, Y. (2013). Parameter analysis of the radial lip seal by orthogonal array method. *Tribology International*, *64*(2), 96–102.

Labib, A. W., Keasberry, V. J., Atkinson, J., & Frost, H. W. (2011). Towards next generation electrochemical grinding controllers: A fuzzy logic control approach to ECM. *Expert System on Application*, *38*(4), 7486–7493.

Lee, Y., Filliben, J. J., Micheals, R. J., & Phillips, P. J. (2013). Sensitivity analysis for biometric systems: A methodology based on orthogonal experiment designs. *Computer Vision and Image Understanding*, *117*(5), 532–550.

Liang, Z., Liu, X., & Tao, J. (2012). Fuzzy performance between surface fitting and energy distribution in turbulence runner. *Scientific World Journal*, *25*(10), 100–113.

Liang, Z., Liu, X., & Ye, B. (2013). Performance investigation of fitting algorithms in surface micro-topography grinding processes based on multi-dimensional fuzzy relation set. *International Journal of Advanced Manufacturing Technology*, *67*(7), 2779–2798.

Liang, Z., Liu, X., & Ye, B. (2014). Fuzzy evaluation of performance influence between surface fitting algorithms and turbulence kinetic energy distribution on runner section. *Arabian Journal for Science and Engineering*, *39*(1), 2339–2351.

Liang, Z., Liu, X., Zhou, J., & Liao, S. (2016). Video tracking for high-similarity drug tablets based on reflective energy intensity matrix and fuzzy recognition system. *Proceedings of the Institution of Mechanical Engineers Part H: Journal of Engineering in Medicine*, *230*(3), 211–229.

Liang, Z., Xie, B., Liao, S., & Zhou, J. (2015). Concentration degree prediction of AWJ grinding effectiveness based on turbulence Characteristics and the improved ANFIS. *International Journal of Advanced Manufacturing Technology*, *80*(5), 887–905.

Liang, Z. W., Ye, B. Y., & Wang, Y. J. (2012). Three-dimensional fuzzy influence analysis of fitting algorithms on integrated chip topographic modeling. *Journal of Mechanical Science and Technology*, *26*(10), 3177–3191.

Maher, I., Ling, L. H., Sarhan, A. A. D., & Hamdi, M. (2015). Improve wire EDM performance at different machining parameters–ANFIS modeling. *IFAC-PapersOnLine*, *48*(1), 105–110.

Mohamad, A., Zain, A. M., Bazin, N. E. N., & Udin, A. (2015). A process prediction model based on Cuckoo algorithm for abrasive waterjet machining. *Journal of Intelligent Manufacturing*, *26*(6), 1247–1252.

Muhammad, N., Manurung, Y. H. P., Jaafar, R., Abas, S. K., Tham, G., & Haruman, E. (2013). Model development for quality features of resistance spot welding using multi-objective Taguchi method and response surface methodology. *Journal of Intelligent Manufacturing*, *24*(6), 1175–1183.

Nagesh, S., Narasimha Murthy, H. N., Ratna Pal, M., & Krishna, B. S. S. (2015). Influence of nanofillers on the quality of CO_2 laser drilling in vinylester/glass using orthogonal array experiments and grey relational analysis. *Optics & Laser Technology*, *69*(5), 23–33.

Nguyen, T., Shanmugam, D. K., & Wang, J. (2008). Effect of liquid properties on the stability of an abrasive waterjet. *International Journal of Machine Tools and Manufacture*, *48*(10), 1138–1147.

Odior, A. (2013). Application of neural network and fuzzy model to grinding process control. *Evolving Systems*, *4*(3), 195–201.

Phootrakornchai, W., & Jiriwibhakorn, S. (2015). Online critical clearing time estimation using an adaptive neuro-fuzzy inference system (ANFIS). *International Journal of Electrical Power & Energy Systems*, *73*(2), 170–181.

Prakash, S., Lilly Mercy, J., Teja, P. V. S., & Vijayalakshmi, P. (2014). ANFIS modeling of delamination during drilling of medium density fiber (MDF) board. *Procedia Engineering*, *97*(5), 258–266.

Sarkheyli, A., Zain, A. M., & Sharif, S. (2015). A multi-performance prediction model based on ANFIS and new modified-GA for machining processes. *Journal of Intelligent Manufacturing*, *26*(4), 703–716.

Sarkheyli, A., Zain, A. M., & Sharif, S. (2015). Robust optimization of ANFIS based on a new modified GA. *Neurocomputing*, *166*(6), 357–366.

Schwartzentruber, J., & Papini, M. (2015). Abrasive waterjet micropiercing of borosilicate glass. *Journal of Materials Processing Technology*, *219*(5), 143–154.

Sedighi, M., & Afshari, D. (2010). Creep feed grinding optimization by an integrated GA-NN system. *Journal of Intelligent Manufacturing*, *21*(6), 657–663.

Sevil Ergur, H., & Oysal, Y. (2015). Estimation of cutting speed in abrasive water jet using an adaptive wavelet neural network. *Journal of Intelligent Manufacturing*, *26*(2), 403–413.

Shabgard, M. R., Badamchizadeh, M. A., Ranjbary, G., & Amini, K. (2013). Fuzzy approach to select grinding parameters in electrical discharge grinding (EDM) and ultrasonic-assisted EDM processes. *Journal of Manufacture System*, *32*(5), 32–39.

Srinivasu, D. S., & Axinte, D. A. (2014). Surface integrity analysis of plain waterjet milled advanced engineering composite materials. *Procedia CIRP*, *13*(6), 371–376.

Tangwarodomnukun, V., Wang, J., Huang, C. Z., & Zhu, H. T. (2014). Heating and material removal process in hybrid laser-waterjet ablation of silicon substrates. *International Journal of Machine Tools and Manufacture*, *79*(4), 1–16.

Teimouri, R., & Baseri, H. (2015). Forward and backward predictions of the friction stir welding parameters using fuzzy-artificial bee colony-imperialist competitive algorithm systems. *Journal of Intelligent Manufacturing*, *26*(2), 307–319.

Teimouri, R., Baseri, H., & Moharami, R. (2015). Multi-responses optimization of ultrasonic machining process. *Journal of Intelligent Manufacturing*, *26*(4), 745–753.

Yusup, N., Sarkheyli, A., Zain, A. M., Hashim, S. Z. M., & Ithnin, N. (2014). Estimation of optimal machining control parameters using artificial bee colony. *Journal of Intelligent Manufacturing*, *25*(6), 1463–1472.

Zhang, T., Liu, X., Sun, F., & Zhang, Z. (2015). The deposition parameters in the synthesis of CVD microcrystalline diamond powders optimized by the orthogonal experiment. *Journal of Crystal Growth*, *426*(5), 15–24.